Optical Chemical Sensors

Colette McDonagh, Conor S. Burke, and Brian D. MacCraith

Chem. Rev., **2008**, 108 (2), 400-422 • DOI: 10.1021/cr068102g

Optical Chemical Sensors

Colette McDonagh,[†] Conor S. Burke,[‡] and Brian D. MacCraith*,[†]

Biomedical Diagnostics Institute, Dublin City University, Glasnevin, Dublin 9, Ireland and Optical Sensors Laboratory, National Centre for Sensor Research, Dublin City University, Glasnevin, Dublin 9, Ireland

Received July 12, 2007

Contents

* To whom correspondence should be addressed. Phone: +353 (0)1 7005299. E-mail: Brian.MacCraith@dcu.ie.
[†] Biomedical Diagnostics Institute, Dublin City University.
[‡] National Centre for Sensor Research, Dublin City University.

1. Introduction

The field of optical chemical sensors has been a growing research area over the last three decades. A wide range of books and review articles has been published by experts in the field who have highlighted the advantages of optical sensing over other transduction methods.[1−5] An appropriate definition of a chemical sensor is the so-called "Cambridge definition":[1,6] *Chemical sensors are miniaturised devices that can deliver real time and on-line information on the presence of specific compounds or ions in even complex samples.*

Figure 1 shows a schematic of a sensor system, illustrating the three main elements, the sample (or analyte), transduction platform, and signal-processing step. Optical chemical sensors employ optical transduction techniques to yield analyte information. The most widely used techniques employed in optical chemical sensors are optical absorption and luminescence, but sensors based on other spectroscopies as well as on optical parameters, such as refractive index and reflectivity, have also been developed. This review will deal mainly with the transduction stage in Figure 1. There will be only limited discussion of sample preparation/enrichment and signal-processing techniques.

Recent developments in the field have been driven by such factors as the availability of low-cost, miniature optoelectronic light sources and detectors, the need for multianalyte array-based sensors particularly in the area of biosensing, advances in microfluidics and imaging technology, and the trend toward sensor networks. In the case of luminescence-based sensors, direct intensity detection has been replaced in many applications by lifetime-based sensing, often using sophisticated phase-based techniques.

This review will focus on developments in optical chemical sensing over the last 10 years with major emphasis placed on the literature from 2000 to the present day. Recent novel developments will be highlighted, and future trends will be discussed. While the optical principles used in chemical sensing have not changed substantially over the years, in many cases the transduction platforms have changed considerably, yielding sensors with vastly improved performance, the most relevant performance parameters being sensitivity, stability, selectivity, and robustness.

The structure adopted for this review is shown in Figure 2. Because of the important role played by the sensor platform in current sensor developments, this review begins with a section on different platforms and platform technologies. This section includes a description of waveguide sensor technology, including fiber-based and planar waveguide systems. Refractometric platforms are also dealt with here as are interferometric sensors.

10.1021/cr068102g CCC: $71.00
Published on Web 01/30/2008

Colette McDonagh studied undergraduate physics at the National University of Ireland in Galway and was awarded her Ph.D. degree in Physics from Trinity College, Dublin, in 1980. After postdoctoral work at Trinity College and the Department of Applied Science at the University of California, Davis, she took up an academic position in the School of Physical Sciences at Dublin City University. She currently holds the position of Associate Professor, and her research interests include development of sol–gel-based optical sensors for environmental monitoring, luminescence-based optical biosensors, and development of strategies for luminescence enhancement in biochips including metal-enhanced luminescence and high-brightness nanoparticles.

Conor S. Burke received his B.Sc. (Hons.) degree in Physics with French from Dublin City University in 1999. In the same year, he started his Ph.D. studies with the Optical Sensors Laboratory in the School of Physical Sciences at Dublin City University under the supervision of Professor Brian MacCraith. He was awarded his Ph.D. degree in 2004 with a thesis entitled "Development of microfabricated optical chemical sensor platforms using polymer processing technology". His work involved development of both colorimetric and fluorometric chemical sensors based on novel, enhanced optical platforms using polymer microprocessing technology. Since then, he has worked as a postdoctoral researcher at the National Centre for Sensor Research, Dublin City University, where his primary research interests include development of novel optical sensors for breath monitoring and environmental applications.

Brian MacCraith is Director of the Biomedical Diagnostics Institute (BDI) at Dublin City University. The BDI is a Science Foundation Ireland (SFI) Centre for Science, Engineering & Technology (CSET) focused on developing the underpinning science leading to next-generation biomedical diagnostics. Established in October 2005, the BDI is an academic–industry partnership involving six industrial and four academic partners and has been funded for 5 years in the first instance. The funding awarded to the BDI includes over 6 million euros from its industry partners and 16.5 million euros from SFI. He was founding Director of the National Centre for Sensor Research at Dublin City University and held this position from its establishment in October 1999 until the establishment of the BDI. Currently, the NCSR comprises over 200 full-time researchers working on the fundamental science and applications of chemical sensors and biosensors. With a strong track record and international reputation in the field of optical chemical sensors and biosensors, he has published widely (over 150 publications) on these topics as well as developing significant Intellectual Property.

In general, optical chemical sensors may be categorized under the headings of direct sensors and reagent-mediated sensors. In a direct optical sensor, the analyte is detected directly via some intrinsic optical property such as, for example, absorption or luminescence. In reagent-mediated sensing systems, a change in the optical response of an intermediate agent, usually an analyte-sensitive dye molecule, is used to monitor analyte concentration. This latter technique is useful particularly in the case where the analyte has no convenient intrinsic optical property, which is the case for many analytes. Section 3 of this review deals with direct optical sensing using a range of optical parameters. This section deals exclusively with direct spectroscopic sensing,

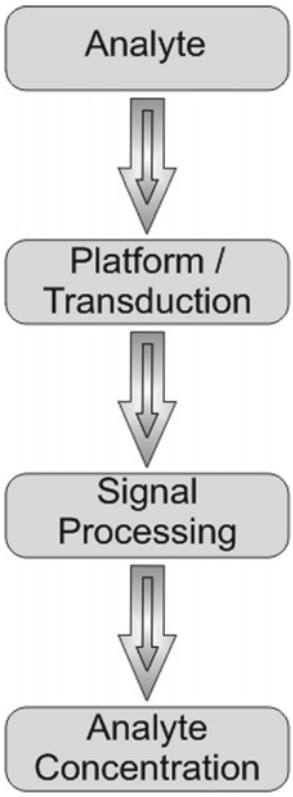

Figure 1. Principal stages in the operation of a sensor.

including infrared (IR) and ultraviolet (UV) absorption techniques, direct fluorescence measurements, as well as Raman and surface-enhanced Raman spectroscopy (SERS). The section on infrared absorption includes a brief discussion of sensing based on the relatively newly developed quantum cascade lasers (QCL). Direct refractometric sensing is

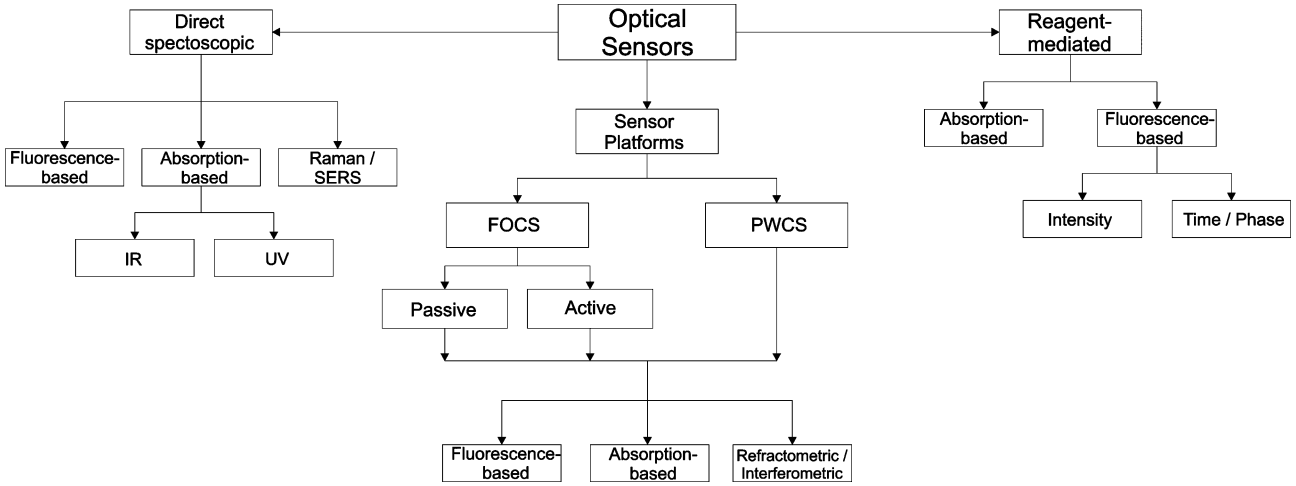

Figure 2. Structure of review.

discussed in section 2. Section 4 on reagent-mediated sensors includes a discussion of analyte-sensitive reagents and associated immobilization approaches, especially those based on polymer and sol−gel matrices, and is followed by a comprehensive overview of recent developments in absorption- and luminescence-based sensors. This review does not contain formal sections on optical biosensors or surface-plasmon-resonance (SPR) based sensors as these topics are dealt with in separate review articles in this issue. However, throughout this review, examples of biosensor applications are given where appropriate, which is a reflection of the current predominance of optical biosensors in sensor research and the overlap between chemical sensing and biosensing.

2. Sensing Platforms

2.1. Introduction

The successful development of an optical chemical sensor is intrinsically linked to the nature of the physical platform on which it is based. When careful consideration of the transduction mechanism dictates the design of the sensor platform, this leads to development of highly efficient integrated optical sensors that combine light delivery/collection with intrinsic sensing functionality. This section will present an overview of optical chemical sensor platforms with an emphasis on innovations in platform design during the past decade. In order to lend clarity to the discussion, the various types of sensor platform are grouped according to the underlying waveguide geometry on which the sensor is based, e.g., optical fiber based or planar, with further differentiation achieved according to the transduction mechanism employed by the sensor.

2.2. Fiber Optic Sensor Platforms

The optical fiber is arguably the most exploited platform in the development of optical chemical sensors, a fact that is reinforced by the sheer volume of publications reporting such systems (over 2500 in the past 10 years). Indeed, this area of sensor research alone merits the publication of regular reviews of the field.[5] Given the scope of fiber optic chemical sensor (FOCS) development, it is difficult for any review of the field to be completely exhaustive. This section will cover the principal fiber optic configurations and sensing schemes that are currently driving sensor research in this area. The scope of this discussion will be limited to sensing strategies that are not the subject of other reviews in this issue. With this in mind, fiber optic sensors that utilize surface plasmon resonance (SPR) techniques and quantum-cascade laser (QCL) spectroscopy or those used to produce high-density sensor arrays will not be described in any great detail, except where such sensors are illustrative of a more general sensing configuration or strategy.

While there exists a multitude of FOCS, the physical configurations employed are relatively few in number, with most sensors falling under one of the fiber categories illustrated in Figure 3, e.g., standard (unmodified) fiber, declad, active cladding, fiber bundle, bifurcated fiber bundle, U-bend, or tip based. In some cases, these configurations are combined in a single sensor, i.e., a standard fiber with a modified tip or a U-bend fiber with an active cladding. A significant fraction of the sensors reviewed here utilize one or more of these configurations/modifications.

In this section, FOCS are classified according to the role played by the fiber in the operation of the sensor, i.e., passive or active. The fiber's role is considered to be passive if the sensor response is not linked in any way to an intrinsic change in the optical properties of the fiber, which acts merely to transport the optical signal to and from the sensing environment. An active FOCS utilizes a fiber that has been modified so as to impart intrinsic analyte sensitivity to the fiber, for example, by doping the fiber cladding with an analyte-sensitive indicator. In this manner, the optical properties of the fiber are in some way modulated by the presence of the analyte. Passive and active systems are treated separately in the following subsections.

2.2.1. Passive FOCS

A wide variety of passive FOCS have been developed over the past two decades, with perhaps the most prevalent example being that of the fiber-coupled spectrometer. However, only those systems developed within the past decade will be reviewed here. A passive FOCS commonly takes the form of a separate sensor element that is interrogated in some fashion by the fiber optic assembly. Several configurations are typically used to achieve this.

The reflectance-based configuration is common in the development of colorimetric or absorption-based FOCS. A typical embodiment of such a sensor comprises an analyte-sensitive material (typically deposited on a planar support) that changes color upon interaction with the analyte of

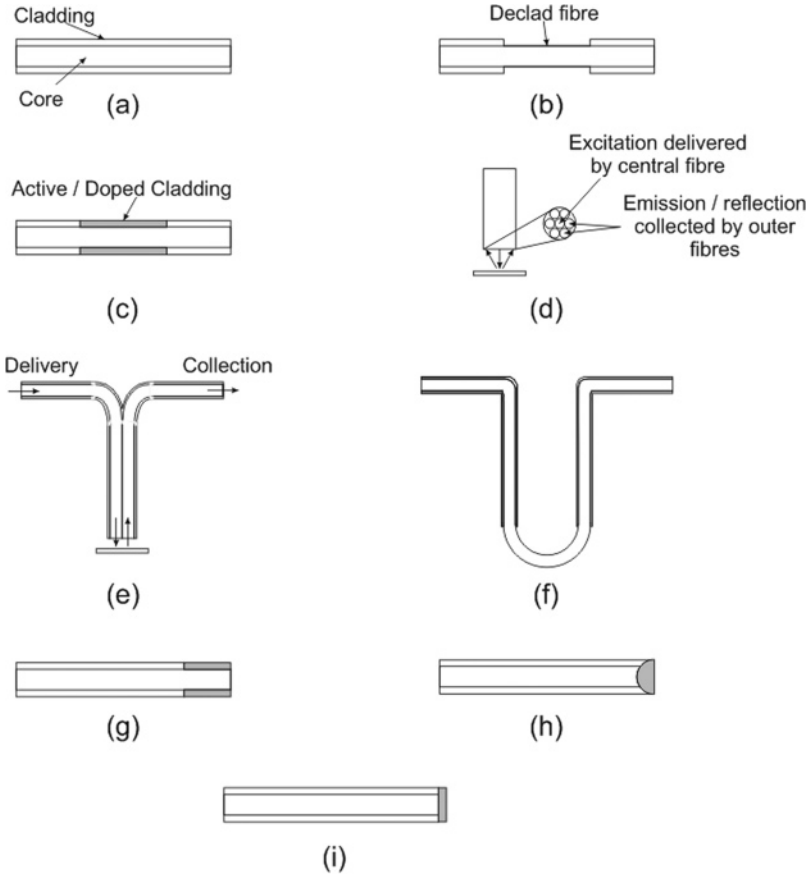

Figure 3. Commonly used configurations for FOCS: (a) unmodified; (b) declad; (c) active or doped cladding; (d) fiber bundle; (e) bifurcated fiber bundle; (f) U-bend (shown declad); (g−i) tip based ((g) tip with active cladding, (h) etched tip, (i) modified end-face).

interest and a fiber bundle (as shown in Figure 3(d)) that is used to deliver light to this material and collect the reflected light. In normal operation, the light is delivered to the analyte-sensitive component via the central fiber in the bundle and the reflected light is collected by the outer fibers, which are arranged around the central fiber. Changes in the color (i.e., the absorption coefficient at a particular wavelength) of the sensor material are detected as changes in the intensity of the reflected light. Such sensor configurations benefit from the commercial availability of fiber bundles (as standard reflectance probes) in addition to the relatively simple optical setup. A reflectance-based system has been used in the development of a sensor for amine vapors based on silica microspheres coated with the pH indicator Bromocresol green.[7] A bifurcated fiber bundle (see Figure 3(e)) has been used in a similar fashion for detection of sulfur dioxide by an organopalladium complex encapsulated in a PVC membrane.[8]

However, the use of a reflectance-based configuration is not limited to detection of analytes by colorimetric means. The same fiber bundles can equally be applied to the excitation and detection of fluorescence. In the case of the fiber bundle depicted in Figure 3(d), the central fiber delivers the excitation light to the external sensor element and the outer fibers are used to collect and transport the emitted fluorescence to a suitable detector. This configuration has been applied to detection of dissolved oxygen.[9]

The bifurcated fiber bundle can be used to deliver excitation light with one fiber and collect the excited fluorescence with the second. This configuration has been used extensively for the fluorescence-based detection of a variety of analytes including oxygen,[10] iodine,[11] 2,6-dinitrophenol,[12] pH,[13] and chloride.[14]

Transmission-based configurations are also commonly employed in the development of FOCS, but in recent years, research has moved away from the conventional configuration employed in many spectrometers, which sees two fibers aligned on opposing sides of a solid sensor element or optical cuvette. While current work still involves the use of fibers that are aligned in such a manner, the sensor element that is interrogated has seen some changes. A subnanoliter spectroscopic gas sensor has been developed. This consists of input and output fibers that are inserted into a fused silica capillary, which acts as a transmission cell for gaseous samples (in this case acetylene) that can be detected using an infrared source.[15] A similar configuration was employed by Eom et al. in the development of a dual-wavelength measurement system for refractive index and turbidity compensation in liquid flow systems.[16] In that case, a length of Teflon tubing played the role of transmission cell and the input/output fibers were used to transport visible light signals from two LED sources, one blue ($\lambda_{peak} = 468$ nm) the other red ($\lambda_{peak} = 621$ nm), to a photodiode detector. In this case, the red LED was used to provide a reference signal.

Such configurations are not limited to cylindrical sample cell geometries. A variety of planar (passive) fiber-coupled sensor platforms have arisen in recent years due to the emergence of microfluidic systems as technology platforms and, in particular, the drive to develop opto-fluidic sensor chips that provide integrated, on-chip optical coupling and detection. One example of this recent trend is a PDMS-based microflow cytometer that incorporates grooves for several

optical fibers positioned at different angles on either side of a flow channel that can be used to excite and detect fluorescence from particles within the channel in addition to scattered light detection.[17] A second PDMS-based device has been developed that utilizes fiber alignment grooves with integrated 2D lenses on either side of a microfluidic channel for fluorescence detection.[18] While these two examples exploit fluorescence detection, the optical configurations used are also inherently suited to transmission-based sensing strategies. Many opto-fluidic microsystems make use of fiber coupling to fulfill either the role of light delivery or light collection but not necessarily both. Yang et al. reported a LED-based capillary electrophoresis system that employs fiber optic detection of the LED-induced fluorescence from within a fused silica capillary.[19] A PDMS microchip for the fluorescence-based detection of human serum albumin has also been described.[20] This system employs an organic LED (OLED) as an excitation source and uses an integrated optical fiber to transport the fluorescence signal to a spectrometer. Chabinyc et al. described development of an integrated, PDMS-based microfluidic system for fluorescence detection that uses a fiber-coupled LED to excite fluorescence from within the microchannels of the system while employing a microavalanche photodiode, encapsulated within the chip, as a photodetector.[21] These examples serve to highlight the importance of optical fibers in rendering these increasingly important platforms optically addressable at a localized level.

2.2.2. Active FOCS

In this section, active FOCS are further categorized under one of three headings, which reflect the transduction mechanism employed: (1) fluorescence based, (2) absorption based (colorimetric and spectroscopic), and (3) refractometric.

(1) Fluorescence-Based Active FOCS. In order to transform a standard optical fiber into an intrinsically fluorescence-based optical chemical sensor, it is necessary to impart analyte-sensitive fluorescence to the fiber in some manner. This is done through addition of fluorescent indicator molecules to the fiber platform. This may be achieved by replacing the cladding of the fiber over a portion of its length with a solid matrix that contains the fluorescent compound, a process that involves removing a portion of the original cladding of the fiber and coating the declad region with a liquid sensor material, which is subsequently cured to form a solid, fluorescent cladding (Figure 3c). A slight variation of this involves coating the declad, distal tip of the fiber with the sensor material (Figure 3g). In some instances, the distal tip may be chemically etched and the fluorescent material deposited within the etched cavity (Figure 3h), while yet another variation involves doping the fiber with the fluorescent material during the fiber fabrication process. However, the latter approach is rarely employed due to its adverse effect on the guiding properties of the fiber.

A variation of the fluorescent cladding configuration was employed by Ahmad et al., who described a system based on two "positive" fibers attached to either end of a "negative" fiber.[22] The system actually consisted of a single fiber, which was declad for a portion of its length and then coated along that portion with a solution of rhodamine 6G in glycerol. The higher refractive index of the glycerol relative to the silica core of the fiber caused any light guided within the fiber to leak out, making this the negative fiber component of the system, while the clad portions on either side of this section constituted the positive (i.e., guiding) fibers. The excitation light that leaked out from the negative fiber induced fluorescence from the rhodamine 6G in the glycerol film, which was coupled into the output positive fiber for detection.

Park et al. described development of fiber optic sensors for detection of inter- and intracellular dissolved oxygen (DO) that utilize "pulled tip" fibers.[23] These are multimode fibers, the tips of which have been pulled down to submicrometer dimensions and then dip coated with a liquid PVC matrix incorporating two luminescent dyes, one that is oxygen sensitive and the other acting as a reference.

A similar configuration was employed by Preejith et al. in the realization of a tapered fluorescent fiber optic evanescent wave-based sensor for serum protein.[24] In that work, a fiber was declad over a length of 5 cm from its end and the declad region was then contoured to produce a tapered fiber tip. The tip was then coated with a sol−gel layer in which the fluorescent complex NanoOrange was encapsulated. Evanescent wave excitation of fluorescence was employed for detection of serum albumin. Both this system and the previous one described by Park et al. differ from that produced by Ahmad et al. in that the latter system does not employ evanescent wave interrogation of the fluorescent cladding, but all three systems demonstrate the use of such a cladding or sensing layer in the production of an active FOCS.

Another example of an active, fluorescence-based FOCS is the platform of Walt et al., which centers on development of high-density fiber bundles for fluorescence-based sensing.[25,26] While this is a high-density array-based platform, it also demonstrates the use of chemical etching to transform the distal tip of a fiber into a well, which can be filled with a fluorescent material. In this case, the fluorescent probe takes the form of suitably functionalized microspheres that are distributed into individual microwells (which correspond to the etched distal tips of individual fibers in a high-density fiber bundle) and can bind specific, fluorescently labeled biomolecules for fluorescence detection in a highly parallel format.

(2) Absorption-Based Active FOCS. Absorption-based optical sensors can be colorimetric or spectroscopic in nature. Colorimetric sensors, as the name would suggest, are based upon detection of an analyte-induced color change in the sensor material, while spectroscopic absorption-based sensors rely on detection of the analyte by probing its intrinsic molecular absorption. FOCS that utilize these techniques have been modified in order to facilitate the interaction of the light guided within the fiber with either the color-changing indicator or the analyte itself, depending on the nature of the sensor.

Both colorimetric and spectroscopic platforms will be discussed in this section, but it will become clear that some of the fiber configurations described for fluorescence-based sensors are equally useful for development of both colorimetric and spectroscopic sensors. Indeed, the modified cladding configuration described above has been used extensively in a number of modes for development of absorption-based sensors, and it should be stressed that only some of the more recent representative examples of such work are reported here.

Recent examples include development of sensors for ammonia (concentration range 0.03−1%),[27] pH,[28,29] and ethanol.[30] In some cases the sensor consisted of a dye-doped

section of fiber cladding that was interrogated by the evanescent field of the guided light,[27] while in other cases a U-bend configuration was also used in conjunction with the dye-doped cladding in order to increase the interaction of the evanescent field with the analyte-sensitive reagent, thereby enhancing device sensitivity.[28] The U-bend configuration was also used in conjunction with a declad section of fiber for spectroscopic monitoring of ethanol.[30] In this case, a dye-doped cladding was not required as the sensor was being used to probe the intrinsic absorption of ethanol molecules in solution and it was necessary merely to remove the cladding from the section of the fiber forming the U-bend in order to yield a sensor element. This work actually described a distributed sensor network and utilized optical time domain reflectometry (OTDR) to interrogate a series of U-bend probes along a 1 km length of fiber. In a recent review of fiber optic sensors, James and Tatam described the development of a Langmuir−Blodgett (LB) film-based sensor for pH.[29] This was fabricated by deposition of a LB film onto a side-polished optical fiber and is another example of a modified cladding-type sensor. With this platform, it was possible to monitor pH-induced changes in the absorption of the LB film at 725 nm, thereby providing the basis for the pH sensor.

Refractometric FOCS. A range of refractometric FOCS has been developed in the past decade that involves addition of refractive index-sensitive optical structures to the optical fiber. Such structures include fiber Bragg gratings (FBG's), Fabry−Perot cavities, and metal films for SPR measurements.

FBG's are written into photosensitive optical fibers (typically germanosilicate fibers) using a suitable laser light source. An interference pattern is produced by passing the laser output through a phase mask or splitting and recombining the laser beam. The fiber is exposed to this pattern, which causes a local modulation of the refractive index of the fiber that matches the pitch of the interference pattern. This refractive index modulation is known as a FBG, and its sensing capabilities derive from the dependence of the Bragg wavelength (and, therefore, the transmission of the grating) on the period of the grating and the effective refractive index, N_{eff}, of the medium. FOCS based on FBG's detect changes in N_{eff} and require that the fiber section bearing the FBG be declad in order to impart sensitivity toward the refractive index of the environment in which the fiber is placed. A twin FBG-based sensor, developed by Sang et al., made use of the second grating in order to provide temperature compensation for the sensor.[31] The device was used to detect different concentrations of sugar and propylene glycol solutions. Long period fiber gratings (LPFG's) are similar structures that are fabricated in the same manner as FBG's but have periods in the range 100−1000 μm. These structures are also refractive index sensitive and have been used for detection of analytes such as sodium chloride,[32] ethylene glycol,[32] and antibodies.[33] Analyte specificity can be imparted to such sensors through deposition of an overlay[29] that possesses its own refractive index response to particular analytes.

A distal tip-based sensor for dissolved ammonia was recently reported by Pisco et al.[34] The sensing element consisted of a tin dioxide (SnO_2) thin film that was deposited onto the distal tip of a fiber by electrostatic spray pyrolysis (ESP). This is an example of a Fabry−Perot interferometric (FPI) FOCS, where changes in the thickness and refractive index of the SnO_2 film at the tip of the fiber and/or changes in the refractive index of the sensing environment cause changes in the reflectivity of the fiber film interface. A zeolite thin-film-based FPI sensor was similarly employed by Liu et al. for detection of organic solvents in water.[35] The optical configuration employed was similar to that of the ammonia sensor mentioned above with the zeolite thin film replacing the SnO_2 layer. An optical humidity sensor for breath-monitoring applications that was also based on a fiber tip FPI configuration was described by Kang et al.[36] In that case, the Fabry−Perot cavity was fabricated through layer-by-layer self-assembly of polyelectrolytes.

Other examples of refractometric FOCS include a sensor for methane developed by Benounis et al., which exploited a cryptophane-doped section of fiber cladding coupled with evanescent wave interrogation.[37] The specific absorption of methane by the cryptophane molecules caused a change in the cladding refractive index, which was indicated by a change in the transmitted optical power of the system. Jung et al. reported a refractive index sensor based on a three-segment optical fiber platform that consisted of a coreless silica fiber (CSF), sandwiched between two standard multimode fibers.[38] The core modes from the first multimode fiber couple to cladding modes in the CSF, which then couple to core modes in the second multimode fiber. The coupling conditions are dependent on the refractive index difference between the CSF and the surrounding medium, thereby providing the system with refractive index detection capabilities.

2.3. Planar Waveguide-Based Sensor Platforms

Compared with FOCS, planar waveguide chemical sensors (PWCS) are a relatively recent innovation in the field of optical chemical sensors. While most FOCS developed to date have adopted one of a small number of relatively conventional configurations (as demonstrated in the previous section), PWCS platforms research is exhibiting rapid growth in terms of innovative design and integration of multiple functionalities onto a single sensor chip. This is largely due to the compatibility of the planar geometry with a range of advanced microfabrication technologies and the ease with which such a sensor geometry can be integrated with microfluidic, lab-on-a-chip systems. Yet another advantage of such a configuration is its robust nature, which, when compared with optical fiber-based systems, is an attractive characteristic when contemplating development of practical sensor devices intended for deployment outside a laboratory environment. These attributes have made planar waveguides an ideal platform for development of integrated optical sensors.

As for the previous section on FOCS, PWCS are categorized here according to the three principal transduction mechanisms employed in this field, i.e., fluorescence, absorption, and refractometry. Before examining each of these areas, it is useful to define the general configuration of a PWCS, the concept of which is illustrated in Figure 4. At its core, a PWCS comprises a planar substrate (e.g., glass, plastic, or silicon) that forms the basis of the sensor chip. In some cases, this substrate acts as the waveguide, while in others an additional waveguide layer is deposited onto the substrate. With regard to the waveguide layer, several configurations have been employed that impart various optical functionalities to the sensor platform, and some of these are reported in the following sections. In many cases,

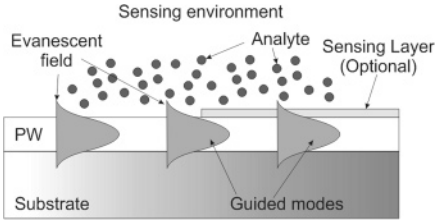

Figure 4. Generalized configuration of a PWCS. In many cases, evanescent wave interactions with the analyte form the basis for the sensor. In some cases, a sensing layer may be employed to facilitate transduction by imparting colorimetric or fluorometric properties to the sensor.

the light that propagates within the waveguide facilitates the operation of the platform as a sensor through the interaction of its evanescent field with the sensing environment above the waveguide. However, this is not always the case, and examples of sensors employing interrogation principles other than evanescent field-based techniques are also given in the sections to follow.

2.3.1. Fluorescence-Based PWCS

PWCS based on detection of fluorescence have been developed for a broad range of analytes including oxygen,[39−42] pH,[41] carbon dioxide,[43] and a variety of biological species.[44−46] Many of these systems employ the technique of evanescent wave excitation of fluorescence (also referred to as total internal reflection fluorescence). The sensor configuration is relatively straightforward, consisting of a planar waveguide to which light is coupled using one of a variety of techniques, such as prism coupling, grating coupling, or end-fire coupling. The evanescent field of the guided light extends into the superstrate (i.e., the sensing environment) and induces fluorescence in susceptible molecules located within a distance of typically 100−200 nm from the waveguide surface. Such a technique is particularly well suited to optical biosensing applications due to the high degree of surface selectivity afforded through the use of the evanescent field for excitation purposes.

Chronis and Lee reported development of a total internal reflection-based biochip platform that excites fluorescence from within a microfluidic network using a single reflection,[47] while the platforms described by Rowe-Taitt et al.[45] and Duveneck et al.[46] (the Zeptosens platform) are examples of multiple reflection (i.e., waveguiding based) evanescent wave excitation systems, which are well suited to development of array-type optical sensor chips.

In some cases, the excited fluorescence is detected either above or below the sensor platform, but it is also possible to use the waveguide itself to capture fluorescence for detection at the output end face of the waveguide.[39,42,48] With such a configuration, it is possible to utilize direct excitation of the fluorescence as opposed to evanescent wave excitation, which results in higher signal levels and improved sensor performance, while improving the inherent ability of the platform to discriminate between the excitation light and the fluorescence.[39,48] Zourob et al. reported an alternative configuration, based on a metal-clad leaky waveguide platform, that also affords enhanced interrogation of the sensing medium, and this system can equally be applied to absorption-based or refractometric sensing schemes[49](Figure 5a,b).

2.3.2. Absorption-Based PWCS

One of the most prevalent examples of absorption-based PWCS platforms is that based on evanescent-wave absorption. The configuration is similar to that described for evanescent-wave excitation-based fluorescence sensors. In this case, the sensing functionality comes about due to changes in the absorption coefficient of the sensing environment. Such changes result in more or less absorption of the evanescent field intensity by the environment, which is reflected as a change in the detected output intensity of the sensor. Sensing layers that are doped with colorimetric, analyte-sensitive indicators can be deposited onto the upper surface of the waveguide, and any analyte-induced color changes can be probed by the evanescent field of a suitable light source (i.e., one that is spectrally matched to the indicator used). In cases where the analyte is detected using direct spectroscopic or refractometric techniques, such a sensing layer may not be necessary, although transparent enrichment layers with high permeability coefficients for the analyte(s) of interest are sometimes employed. PWCS that utilize thin-film-based sensing layers have been employed for detection of analytes such as gaseous ammonia,[50,51] pH,[52] iodine,[53] and water vapor.[54]

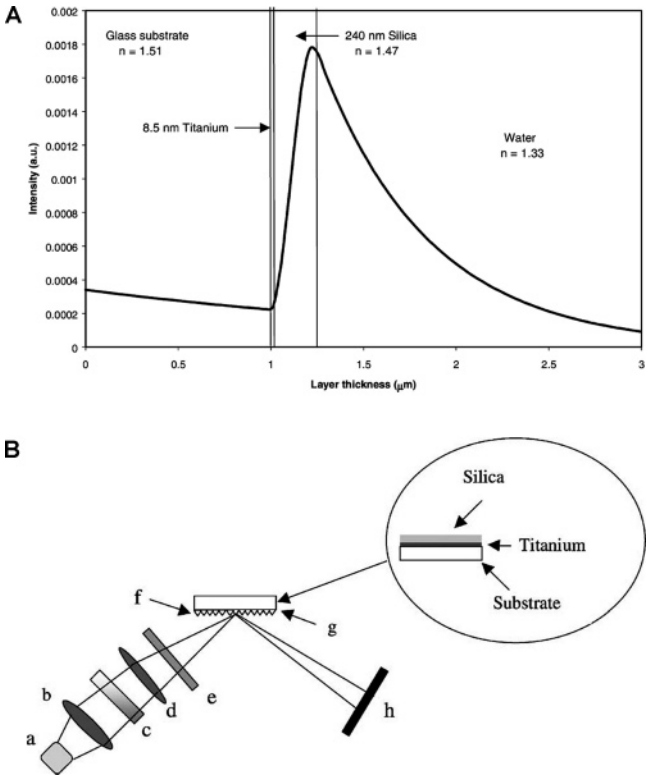

Figure 5. (A) Mode profile of a metal-clad leaky waveguide covered by water at a wavelength of 620 nm using a 1 mm glass substrate. (Reprinted with permission from ref 49. Copyright 2003 Elsevier Science B.V.) (B) Instrumental set up for optical sensor based on a metal-clad leaky waveguide using a (a) 473 nm solid-state laser or 610 nm LED, (b) collimating lens, (c) filter, (d) cylindrical lens, (e) polarizer, (f) grating, (g) sensor chip, (h) linear CCD detector or photomultiplier detector. (Reprinted with permission from ref 49. Copyright 2003 Elsevier Science B.V.)

However, in recent years, a number of platforms have been developed that demonstrate a shift away from what might be seen as conventional evanescent wave absorption-based platforms. These platforms typically incorporate design features intended to enhance the interaction of the interrogating light with the sensing environment, thereby improving platform sensitivity. The integrated waveguide absorbance optode (IWAO) developed by Puyol et al. incorporates a PVC-based sensor membrane that is located between two

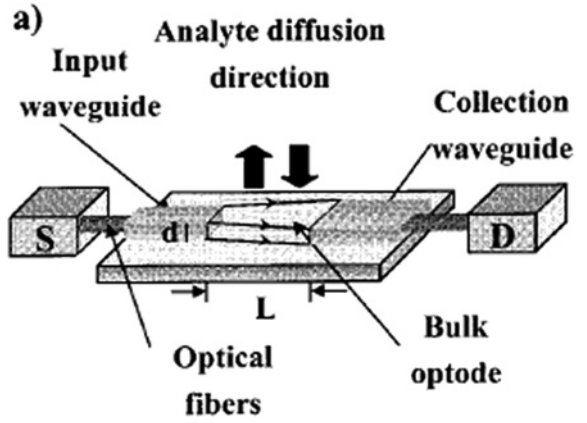

Figure 6. Integrated waveguide absorbance optode (IWAO) configuration developed by Puyol et al. (Reprinted with permission from ref 55. Copyright 1999 American Chemical Society.)

antiresonant reflecting optical waveguides (ARROWs)[55] (see Figure 6). The sensor membrane also serves as a waveguide and transports the interrogating radiation from the input ARROW to the output waveguide. The increased optical path length within the sensing layer provides enhanced sensitivity, and the device was applied to detection of potassium chloride solutions of varying strength.

This configuration was later improved upon to incorporate curved ARROW waveguides and achieved improved sensitivity and response time.[56] Hisamoto et al. reported development of ion-selective optodes[57] that employ a similar strategy in that the sensing layer also serves as the waveguide (referred to as an "active waveguide"). This system is based primarily on a prism-coupled glass platform, which incorporates the PVC-based sensor membrane and has been applied to detection of a variety of analytes including potassium, sodium, and calcium. Qi et al. reported a composite optical waveguide (COWG) platform that consists of a potassium-ion-exchanged (PIE) waveguide onto which a tapered film of bromothymol blue (BTB)—a colorimetric pH indicator—is deposited.[58] The BTB film acts as a single-mode waveguide, and the sensor achieved a limit of detection (L.O.D.) of 1 ppb ammonia. Other systems that exploit enhanced interrogation of the sensing medium include the previously mentioned metal-clad leaky waveguide platform developed by Zourob et al.,[49] while Burke et al.[59] reported an injection-moulded waveguide platform that facilitated enhanced interrogation of a thin absorbing sensing layer through correct choice of the incident angle of interrogation, which was dictated by the design of integrated refractive optical elements.

2.3.3. Refractometric PWCS

PWCS designed to measure refractive index changes represent one of the most extensively developed types of planar waveguide platforms. These systems exploit techniques such as interferometry, surface plasmon resonance, and light-coupling strategies to transduce refractive index changes. Comprehensive reviews of integrated optical chemical sensors based on such devices have recently been published by Lambeck[60] and Gauglitz.[61] A representative cross-section of cutting-edge sensor technology in this field will be delivered here, but readers should refer to these reviews for further reading on this sector of sensor technology. Sensors based on surface plasmon resonance (SPR) are perhaps the most widely known examples of refractometric optical sensor platforms. However, this family of sensors will not be discussed here as it is the subject of a separate review in this issue.

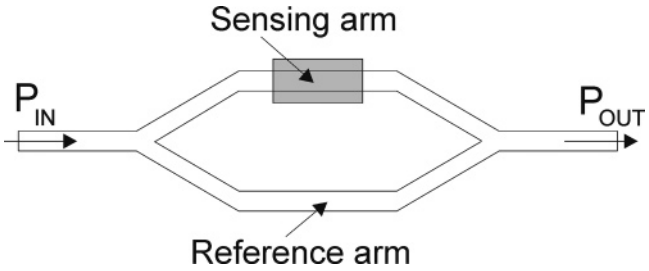

Figure 7. Schematic of a Mach−Zehnder interferometer.

The first branch of refractometric PWCS to be discussed here is that of interferometric sensor platforms. A significant number of refractometric PWCS are based on exploitation of interferometric techniques, and one of the most commonly employed optical configurations is the Mach−Zehnder interferometer (MZI), shown in Figure 7.

The MZI consists of a single-input waveguide whose transported optical power is split equally between two parallel waveguide branches using a Y-splitter. A second Y-splitter is used to recombine the optical signals from both branches into a single-output waveguide, at the end of which the output power is measured using a suitable photodetector. For the purposes of chemical sensing applications, one of the waveguide branches is either coated with a sensor membrane or exposed to the sensing environment while the other unmodified branch serves as a reference waveguide. Changes in the refractive index of the sensing layer/environment influence the effective refractive index, N_{eff}, in the sensing channel, which induces a phase shift in the optical signal that propagates through this channel. Upon recombination, interference of the two optical signals (i.e., sensor and reference) occurs and the measured output power changes depending on the phase shift between these two signals. In the recent review by Lambeck, a comprehensive treatment of MZI interferometric platforms has been given, including a discussion of a range of strategies intended to enhance sensitivity and general sensor performance. This involves optimizing parameters such as operating wavelength, interaction length, and, most importantly, the waveguide composition. The MZI configuration has recently been exploited by a number of groups for detection of a variety of chemical and biochemical species.[62−66] Improved performance can be achieved by implementing serrodyne modulation, which involves inserting electro-optical modulators into each branch.[67]

Other interferometry-based PWCS include the Young interferometer,[68−70] the Michelson interferometer,[71] and the difference interferometer (also referred to as a polarimeter).[72−74] These platforms can be described as derivatives of the MZI and operate in an analogous fashion (see ref 53 for further details). Some noteworthy examples are the Young-type interferometer that has been commercialized by Farfield Sensors [www.farfield-scientific.com] and the Zeeman interferometer,[75] which is a variant of the difference interferometer that is capable of resolving refractive index changes on the order of 10^{-8}. In addition, Kribich et al. describe development of a multimode interference (MMI) coupler with tunable sensitivity that has been used to detect changes in relative humidity.[76] This platform consists of single-mode input and output waveguides that are coupled to a central

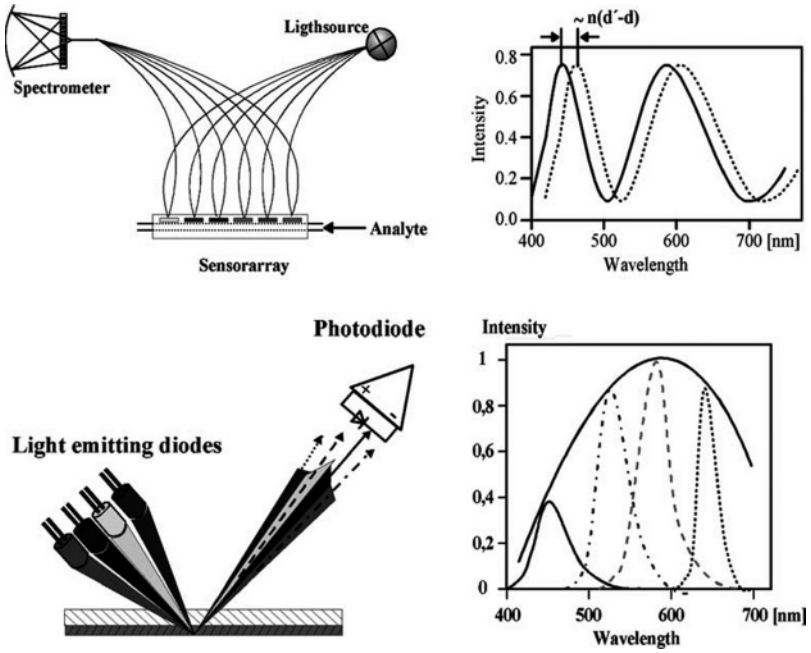

Figure 8. RifS configurations and measurement principle. (Reprinted with permission from ref 61. Copyright 2005 Springer-Verlag.)

multimode waveguide. The field profile within the multimode region is dependent on the refractive index of the superstrate, and changes in this are detected as changes in the output light intensity.

Lavers et al. described a related coupled-waveguide-type refractometer, which consists of a buried, single-mode potassium ion-exchanged (PIE) waveguide in a BK7 glass substrate, onto which a multimode polymer waveguide is deposited by photolithographic means.[51] While this device also exploits the effects of coupling between dissimilar waveguides, it is more properly an example of a resonant-type refractometric PWCS, other examples of which include the resonant mirror platform,[77] metal-clad leaky waveguides,[49,78] and some grating-based devices.[79−81] Other grating-based devices have been developed that rely on the refractive-index- and thickness-dependent nature of diffraction to yield a sensor response that manifests itself as a change in the intensity or spatial distribution of the diffraction pattern.[82−86] Platforms based on this phenomenon are under development by Axela Biosensors [www.axelabiosensors.com], although in that particular case the sensor response is primarily due to changes in the thickness of the receptor layer that defines the diffraction grating as opposed to alterations in refractive index, and the platform is included here in order to illustrate the perceived utility and commercial potential of such a sensor configuration.

Several other noteworthy PWCS platforms have been developed that exploit thickness-sensitive measurement principles, as opposed to refractometry. Reflectometric interference spectroscopy (RIfS),[87] developed by Gauglitz, is one such technique. The principle of RIfS is illustrated in Figure 8 and, in brief, centers on detection of changes in the interference pattern generated by light that is reflected from the interfaces of a thin film deposited on a substrate. Changes in the thickness of the thin film (e.g., due to swelling upon interaction with the analyte of interest) result in a shift in the observed interference pattern, and the technique is capable of resolving a thickness change of 1 pm.

Nikitin et al.[88] exploited the interference pattern generated by light reflected from the upper and lower surfaces of a glass cover slip in the development of the Picoscope. This system measures the correlation signal of two interferometers—the cover slip and a scanned Fabry−Perot interferometer—to monitor changes in the thickness of the cover slip (due, for example, to biomolecular binding events) with a reported resolution of 3 pm. Lambeck et al. proposed three theoretical strip waveguide configurations implemented in SiON technology—segmented, absorptive, and directional coupler based—that are designed to transduce thickness changes through changes in the field profile of the waveguide modes with a calculated resolution of 3×10^{-5} nm.[89]

2.3.4. Light Coupling Strategies for PWCS

An important design consideration in the development of any PWCS is the method by which light is coupled to the sensor platform. The most commonly employed techniques are prism coupling,[49,57,58,77] grating coupling,[45,46,50,69,70,78] and end-fire coupling,[42,55,62,63,65,66,68,72,74−76] with the choice of technique typically involving a tradeoff between fabrication costs, practicality, and sensor performance. The use of prism couplers provides relatively high coupling efficiency but detracts from the cost effectiveness, planarity, and overall robustness of the sensor platform, while end-fire coupling requires extremely precise alignment optics in order to be effective, which is not an attractive feature in a field deployable sensor but is an obstacle that can be overcome by employing fiber-pigtailing strategies (although this makes easy exchange of the sensor element problematic). The use of grating couplers can be seen as a viable alternative as this is a low-cost option that preserves the robustness of the sensor, but the reduced coupling efficiency may adversely affect sensor performance. Some efforts have been made to integrate the coupling functionality into a single chip using polymer microprocessing techniques such as injection molding[59] or hot embossing.[41] These techniques are compatible with the production of integrated grating couplers and refractive/prismatic optical elements that provide adequate coupling efficiency, do not reduce the robustness of the sensor, and also emphasize the trend toward integration of multiple functionalities on a single sensor platform.

2.4. Summary

A range of recently developed optical chemical sensor platforms have been categorized and discussed according to the underpinning waveguide geometry employed. Further categorization was achieved according to the transduction mechanism upon which the sensors were based, and development of a number of highly innovative sensor platforms has been highlighted. This is particularly true of research in the field of planar waveguide-based devices where this robust, microfabrication-compatible geometry has been shown to lend itself well to development of optical chemical sensors having a range of integrated functionalities. However, integration of multiple functionalities (e.g., light delivery and analyte detection capability) is not limited to a planar geometry, as evidenced by the volume of work on active fiber-based sensors. The broad range of exciting developments in the field of optical chemical sensor platform development is indicative of the increasing interest in these devices and an acknowledgment of their effectiveness in providing sensitive, practical sensor solutions for a variety of application areas.

3. Direct Sensors

3.1. Introduction

Direct optical detection involves the measurement of some intrinsic optical property of the analyte. Many direct sensors, for example, gas sensors, measure the intrinsic optical absorption, usually in the infrared (IR), using a variety of techniques including Fourier transform infrared (FTIR) spectroscopy or correlation spectroscopy. A range of optical configurations has been used, from free-space sensors to fiber-based configurations to optical waveguide sensors. Fiber optic and planar waveguide sensing platforms have been discussed in section 2 of this review as well as refractometric platforms such as the Mach Zehnder interferometer. Developments in IR sensing have been driven largely by the emergence of new diode laser sources, for example, QCL lasers. This section includes a comprehensive discussion of direct IR absorption sensing including FTIR-based systems. While a review of QCL-based sensing appears elsewhere in this issue, a short section on this topic is included here under the heading of diode laser-based sensing. A brief section on UV absorption is included, mainly concerned with environmental sensing of organic pollutants. Similarly, direct fluorescence sensing is dealt with mainly in the context of biomedical applications. Recent developments in SERS-based sensing are reported, which reflect the huge growth in this area in the last 10 years.

3.2. Direct Spectroscopic Sensing

3.2.1. Absorption-Based Sensors

IR Absorption. For many applications, spectroscopic detection has been a reliable method of detecting chemical species. IR spectroscopy has been widely used for detection of gases, for example, CO_2, CO, NO_2, NH_3, and CH_4. In its simplest form, the technique involves confining a sample of the gas in an optical absorption cell and measuring the absorption at specific IR wavelengths, which are characteristic of the vibrational modes of the molecule. The system components usually include an IR source, optical filters to select specific absorption wavelengths, and a detector, which is sensitive at the wavelength of interest. Referencing can also be employed using a wavelength that is not absorbed by the analyte molecule. The fundamental vibrational transitions of many molecules of interest occur in the near- and mid-IR, spanning wavelengths from 1 to >10 μm. Gas analysis is becoming increasingly important in control of various industrial processes, for example, in combustion processes and monitoring industrial emissions. The need for environmental control of emissions has also led to development of analyzers to measure the concentration of a variety of gases. Much of this instrumentation is based on near- and mid-infrared absorption spectroscopy.

While conventional IR sensing uses broadband IR sources, recent developments in diode laser technology, including the relatively recent availability of novel QCL sources, have led to development of highly sensitive and selective sensor systems. Fourier transform infrared (FTIR) spectroscopy is also a very powerful analytical tool. Nondispersive infrared (NDIR) sensors are widely used for gas analysis, and many commercially available gas analyzers are based on this principle.

NDIR Sensors. NDIR sensors use band-pass filtering in order to select the specific analyte absorption wavelength as opposed to dispersion by a prism or a grating as employed in a spectrometer. NDIR-based sensors have been developed to monitor CO_2 concentrations in the ocean in order to monitor the effects of increased atmospheric CO_2 on the global carbon cycle. Total inorganic carbon measurement involves acidification of the seawater sample and quantitative measurement of the evolved CO_2. NDIR detection has been found to yield a precision of 0.11−0.25% and an accuracy of ∼0.1% for total inorganic carbon detection.[90,91] Kaltin et al.[92] employed NDIR to measure the extracted CO_2, and the system continually compares the signal to a certified reference material, which constitutes the baseline signal. A precision of ∼0.05% was achieved with an accuracy of ∼0.2%, which was comparable to the performance of the standard colorimetric technique, and the sampling time of 5 min was 3 times faster than the colorimetric method. In order to produce the speed of measurement desired to enable high-speed continuous analysis, Bandstra et al.[93] employed a gas-permeable hydrophobic membrane contactor, which continuously strips the CO_2 out from a flowing stream of seawater. The system continuously quantifies the CO_2 concentration using an NDIR analyzer, which uses a lead selenide detector and broadband blackbody source, yielding an accuracy and precision better than ±0.1% and a response time of 6s.

FTIR-Based Analyzers. FTIR-based sensing is an alternative to NDIR-based analyzers and has advantages for many applications. Current FTIR spectrometers offer precise quantification of a wide range of analytes for concentrations down to single-digit ppb levels and are now available as integrated and relatively compact units compared to the complex and bulky units offered in the past. An FTIR spectrometer consists of an interferometer, usually a Michelson type, which generates an interferogram from the IR emission of the sample and then performs a Fourier transform to obtain the spectrum. The ability of FTIR to measure multiple analytes simultaneously differentiates the technique from NDIR sensors. Castro et al.[94] recently reported the use of FTIR to characterize low-temperature combustion gases in biomass fuels. The spectrometer, operating in absorption mode, was placed in front of an IR source and mounted such

that the optical line of sight was just above the sample, allowing the absorption of the emitted gases to be measured. A high acquisition speed was necessary in order to evaluate temporal evolution of gas concentrations and improve the signal-to-noise ratio. A spectral resolution of 1 cm^{-1} was selected as a compromise between required spectral resolution and acquisition time. The concentration of three gases, CO_2, CO, and CH_4, which are the most important carbon-related products of biomass combustion (shrub species in this case), was measured in situ. These results can contribute to improved modeling of pyrolysis for predicting forest fire behavior.

FTIR has also been used for analysis of vehicular emissions; for example, Reyes et al.[95] monitored a range of pollutants including CO, NO, SO_2, and NH_3 under different driving conditions using a hybrid car. However, no detailed performance parameters were given.

FTIR imaging has been used for high-throughput analysis of processes such as epoxy curing,[96] gaseous or solid-phase reactions,[97] and monitoring of pharmaceutical formulations under different conditions.[98] Chan et al.[98] applied FTIR imaging to the study of the behavior of drug formulations such as ibuprofen as a function of different environmental parameters. They combined a microdrop device with an FTIR imaging system, which consisted of a step scan spectrometer coupled to a macrochamber extension and a 64 × 64 focal plane array (FPA) detector. Spectra were measured with a 16 cm^{-1} resolution and a spectral range of 3950−900 $cm^{-1.}$ They demonstrated for the first time the simultaneous analysis of 100 samples. The system allows fast screening of many formulations under controlled environments. FTIR spectroscopy has been used for on-line monitoring of formaldehyde-based resin synthesis.[99] The system used a FT-NIR spectrometer fiber optic data acquisition, and spectra were collected at 8 cm^{-1} optical resolution. Chemometrics was employed to provide fast and reliable process information on an industrial scale. No sample manipulation was required, and data was acquired in less than a minute.

Diode Laser Sensing Systems. While FTIR is well suited to multicomponent analysis of gases and other chemical species for a range of processes, laser spectroscopy is the method of choice for trace gas analysis because of its higher sensitivity and specificity, which arises when a spectrally narrow laser source probes a narrow absorption feature of the analyte. Werle[100] and Allen[101] produced comprehensive reviews of diode laser-based gas sensor systems for applications such as automated control of industrial processes, environmental monitoring, and combustion process monitoring. The lasers used for gas analysis span the near- and mid-IR spectral regions with wavelengths ranging from 1 to $>2\mu$m for conventional diode lasers and from 2 to $>4\mu$m for recently developed QCL lasers.

Fiber-coupled multiwavelength diode laser sensor systems have been designed which use modulation spectroscopy and multipass absorption cells to increase sensitivity. Wavelength modulation spectroscopy has been used to monitor gas emission in industrial processes.[102] Tunable diode laser absorption spectroscopy (TDLAS) systems, using lead salt lasers which are based on IV−VI semiconductors, have been used to achieve parts per billion detection levels of atmospheric gases, for example, methane.[103] However, these systems require laser cooling and are not suited to unattended routine industrial applications. While lead salt lasers operated at cryogenic temperatures cover the fundamental gas absorption bands required for ultrasensitive gas analysis, near-infrared diode lasers, operated at room temperature, probe mainly the weaker overtone and combination bands of the analyte molecule. Therefore, there is a trade off between sensitivity and convenience of operation. Sensitivity problems can be overcome using appropriate signal processing and double-modulation techniques.[104]

QCL lasers are semiconductor lasers based on transitions in a multiple quantum well heterostructure. The emission wavelength depends mainly on the quantum well thickness rather than on the size of the band gap, as is the case with conventional diode lasers. QCLs operate at wavelengths in the MIR starting at about 3 μm, which match well with the fundamental vibrational absorption bands of many gases and other chemical species in comparison with conventional diode sources where the laser emission generally matches the weaker overtone bands. QCLs operate at near room temperature, produce milliwatts of radiation, and offer the possibility of tailoring the emission wavelength within a broad range of frequencies.[105,106]

The most technologically developed QCLs are based on InGaAs−InAlAs and GaAs−AlGaAs heterostructures.[107] They are usually fabricated as single-mode lasers and often in a distributed feedback (DFB) configuration. QC-DFB lasers are of particular interest for gas sensing as they produce highly monochromatic radiation that is suitable for high-resolution spectroscopy.[108]

The first reports of gas sensing using a CW QC-DFB laser was by Sharpe et al.,[109] where they presented absorption data on NO and NH_3 at low pressure. The first QCL-based system for determination of CO_2 in aqueous solution was reported by Schaden et al.[110] A QCL gas sensor system for measuring trace gases in air was reported by Kosterev.[111] Gases such as CH_4 and N_2O were detected down to ppb levels. A QC-DFB laser system was used to measure ppb levels of NO in vehicle emissions,[112] while high-precision measurements of atmospheric N_2O and CH_4 were reported by Nelson et al.[113] Sensing in liquids has also been reported. A Fabry−Perot QC laser system, consisting of two lasers, one tuned to a water vibration and the second to a water window, was used in a flow injection system equipped with a fiber optic flow cell with an adjustable path length. Adenine and xanthosine were used as test analytes, and the results demonstrated the advantages of QCL lasers in overcoming solvent interference for liquid sensing.[114]

UV Absorption. Direct UV absorption sensing has been used mainly in environmental applications to monitor pollutants such as heavy metals, hydrocarbons, and volatile organic compounds (VOC) in air and water. A sensor to detect Cr(VI) in water that is based on a flexible fused silica capillary and intrinsic evanescent-wave UV absorption of Cr ions in a water sample in the capillary has been reported.[115] A Cr(VI) absorption band peaking at 374 nm was monitored, and a limit of detection of 31 parts in 10^9 was achieved using an absorption path length of 30 m of capillary. The concentrations of ozone and NO_2 in the atmosphere were measured by UV-differential optical absorption spectroscopy (UV-DOAS), and the results were used to evaluate the contribution of NO_2 in limiting ozone formation.[116] The UV-DOAS system used a broad-band xenon source that was placed at a level of 12 m on top of a building, and the detector was placed 150 m away. A premeasured clean-gas reference spectrum was used to generate the differential absorption spectrum. UV-DOAS was

also used to monitor VOCs and aromatic hydrocarbons in ambient air in the vicinity of a refinery.[117] The system detected high levels of benzene and toluene and also monitored seasonal variations in VOC concentrations. UV-DOAS was one of four VOC monitoring techniques used in a field study in Mexico to identify VOCs that were primarily due to vehicle emissions.[118] The data were analyzed to understand the spatial distributions, diurnal patterns, and reactivity of various VOCs. One of the key results of this study was a better understanding of the interaction between vehicular activity and meteorological processes.

3.2.2. Direct Fluorescence Sensing

Direct fluorescence sensing is widely used in biomedical applications. Autofluorescence spectroscopy is a useful tool for noninvasive detection of precancerous development of the epithelium, where most human cancers originate. This fluorescence arises mainly from two intrinsic fluorophores, reduced nicotinamide adenine dinucleotide (NADH) and flavin adenine dinucleotide (FAD). The fluorescence of these species can be used to monitor cell activity. For example, the ratio of free and bound NADH, differentiated by their different lifetimes, is a good indicator of the cell metabolic state. Wu et al.[119] used a time-resolved confocal fluorescence spectroscopy system to study cell metabolism and were able to differentiate between cancerous and normal cells by analyzing the dual-exponential decay of NADH. Depth-resolved fluorescence spectroscopy, using a confocal microscope and multiple excitation wavelengths, was used to study different layers of the epithelium.[120] By exciting at 355 and 405 nm, the system was able to isolate the fluorescence from different sublayers. In particular, the ratio of NADH to FAD fluorescence can be used to indicate the presence of precancerous cells. Autofluorescence patterns have also been used to follow changes in cervical tissue[121,122] and oral tissue.[123] The intrinsic fluorescence of tryptophan has been used to study protein folding and unfolding. Tryptophan fluorescence is very sensitive to the environment, whereby the peak emission wavelength shifts from 308 to 350 nm for the range of protein conformational changes.[124] This spectral behavior has been used to study protein stability[125] and protein aggregation.[126]

Fluorescence can be used to characterize different oils as the fluorescence is dependent on chemical composition. For example, crude petroleum oils have been analyzed using synchronous fluorescence, where both the excitation and emission monochromators are scanned simultaneously, and lifetime measurements were carried out.[127,128] Recently, biocrude oils, derived from seeds, have been analyzed.[129] Synchronous fluorescence has also been used to quantitatively discriminate between virgin olive oil and sunflower oil,[130] and fluorescence spectroscopy combined with artificial neural networks has been used to classify a range of edible oils.[131]

3.2.3. Raman and SERS Sensing

Like IR-based absorption spectroscopy, Raman spectroscopy probes the vibrational energy levels of molecules and therefore can be used as a highly selective technique which will distinguish between similar molecules. The Raman effect occurs when a photon interacts with the vibrational energy levels of a molecule and is scattered.[132] Raman spectroscopy normally requires laser excitation and relies on good optical filtering to separate the scattered photon from the intense incident beam. Unfortunately, Raman scattering cross-sections are very small, many orders of magnitude smaller than fluorescence cross-sections. However, it is still a useful technique for sensing of gaseous and liquid analytes. It has a particular advantage over IR absorption for liquid sensing in that there is no interference from the vibrational spectrum of water. For this reason, Raman is a useful technique for life science applications, including biomedical diagnostics, for example, the study of living cells. Lasers with large spot sizes ($>10\ \mu$m) can be used to study whole cells and tissues. Raman imaging using diffraction-limited spot-size lasers can be used to map the chemical distribution in a cell.[133] Uzunbajakava et al.[134] used a laser with high lateral resolution to map the DNA and RNA distribution in GeLa cells. Principal components analysis of Raman spectra has been used to distinguish between different cancer cells.[135,136] A Raman imaging system, based on fiber optic probes, has been used to image breast tissue.[137] Different tissue features were identified from differences in the Raman spectra. Toxins such as sulfur mustard and ricin have been identified in cells with an identification accuracy of 88.6% and 71.4%, respectively, using Raman spectroscopy.[138]

The disadvantages of conventional Raman, such as the low scattering cross-sections, can be overcome to a large extent using the SERS technique. The strength of Raman scattering from a molecule in close proximity to a nanostructured metal surface can be enhanced by as much as a factor of 10^8, compared to conventional Raman. This surface-enhanced effect is strongest for silver and due to the interaction of the localized surface plasmon, generated at the metal surface, with the vibrational levels of the molecule. The large electromagnetic field generated induces a dipole in the molecule that is adsorbed on the metal surface, hence producing the hugely enhanced Raman signal.[139] The two principal conditions required for SERS to be observed are the presence of a suitable SERS-active nanostructured metal surface and the requirement that the sample under investigation be immobilized on or in close proximity to the surface. In the past, routine application of the technique has been hampered by a poor understanding of the theoretical background and lack of reproducibility of SERS substrate materials. Recently, with advances in materials fabrication and better understanding of the details of the plasmonic interaction, SERS is being increasingly used in diverse fields such as biomedicine and environmental analysis. A number of review articles have been published recently with particular emphasis on biomedical applications of SERS.[140−142] The use of SERS to obtain quantitative in-vivo glucose measurements has been reported,[143] where a suitable SERS surface was achieved using a silver-coated self-assembled monolayer (SAM) of polystyrene nanospheres. The SERS probe was implanted in a rat, and the data obtained agreed well with simultaneous data monitored using a conventional electrochemical glucose sensor. The same substrate has also been used to detect the presence of the chemical warfare agent half-mustard.[139] A combination of near-field scanning optical microscopy and SERS has been used to detect dye-labeled DNA with 100 nm resolution.[144] SERS has been used to detect specific dyes in works of art. Anthraquinone[145] and alizarin dyes have been identified.[146] For the alizarin investigation, silver nanoparticles were deposited directly onto a sample of the painting. The advantage of SERS over conventional Raman was highlighted in this work as strong fluorescence of the dye completely masked the Raman signal,

while in the SERS measurement, the fluorescence was quenched due to the presence of the metal substrate, enabling detection of the enhanced Raman signal. In environmental sensing, a SERS optode has been used to detect polycyclic aromatic hydrocarbons (PAHs) in seawater.[147]

3.3. Summary

This section on direct sensing has focused exclusively on spectroscopic techniques. A short review of the range of IR absorption techniques and configurations used in gas analysis and sensing of organic compounds was given. NDIR- and FTIR-based sensing are both used extensively, FTIR being more appropriate for high-throughput, multianalyte applications. Laser-based systems are more complex and expensive but offer very high sensitivity, allowing detection down to ppb levels. The availability of QCL sources has been a novel development in this area and enables relatively compact, robust systems for use in the field. The recent growth of SERS-based sensing was discussed, and examples of diverse applications, including some biosensing applications, were given.

In summary, it has to be said that, currently, the most widely used direct optical sensing technique is that of IR absorption-based sensing, mainly for gas analysis. For example, of the total commercial gas analyzer market in the United States, NDIR sensors had about a 50% share in 2005. It will be interesting to observe whether this technique still dominates the optical sensing market over the next decade. It will also be interesting to see if the current growth in SERS sensing will be sustained and whether it will lead to commercial sensor systems.

4. Reagent-Mediated Sensors

4.1. Introduction

When an analyte does not exhibit a convenient spectroscopic optical response such as absorption or luminescence, sensing can be achieved by monitoring the optical response of an intermediate species or reagent, whose response is modulated in some way by the presence of the analyte. Reagent-mediated sensing is illustrated very well by the principle of optical oxygen sensing, whereby the luminescence intensity or decay time of an oxygen-sensitive luminescent complex, for example, a ruthenium polypyridyl or a porphyrin complex, is quenched in the presence of oxygen. This enables the oxygen partial pressure to be measured as a function of the intensity or luminescence decay time of the complex. Indirect colorimetric sensors also require an intermediate reagent, for example, many optical pH sensors have been based on monitoring the change in optical absorption of pH indicators such as bromocresol purple. This indirect sensing technique requires the reagent to be immobilized, either in the liquid or in the solid phase, to facilitate interaction with the analyte. In recent years, reagent-based optical sensing has been based mainly on solid-phase immobilization matrices, where the reagent dye can be adsorbed, covalently or ionically attached, or simply encapsulated in a solid matrix that is permeable to the analyte. If the immobilization matrix has the capability of being coated on a substrate in liquid form, as is the case for sol−gel glasses or polymer coatings, a wide range of sensor configurations is enabled including, for example, fiber optic, planar waveguide and array-based sensors. These configurations have already been described in section 2. Section 4.2 of this review will report on the wide range of reagents used in recent years in optical absorption- and luminescence-based chemical sensors, while section 4.3 describes two widely used sensor immobilization matrices, namely, sol−gel and polymer materials. Subsequent sections review the state-of-the-art in absorption- and luminescence-based systems, dealing mainly with work that has been published in this decade.

4.2. Reagents

4.2.1. Reagents for Colorimetric Sensing

Indirect colorimetric pH sensing uses organic pH indicators, the absorbance of which is modified by the pH of the environment. The pK_a of these indicators indicates the center of the measurable pH range, for example, cresol red, bromophenol blue, and bromocresol purple respond to acidic pH (pH < 7), while cresol red, naphtholbenzene, and phenolphthalein respond at basic pH (pH > 7).[148] The relatively narrow pH response range of most of the above dyes has been addressed whereby several indicators with different pK_a values have been combined in one sensor in order to produce a linear pH response over a wide range.[149] Makedonski et al.[150] synthesized new reactive azo dyes for use in pH sensing where the dyes were covalently bound to a polymer matrix for increased sensor stability. Recently, phenolphthalein has been used to monitor the behavior of corrosion-resistant polymers in alkaline solutions in chemical plants.[151]

Since colorimetric CO_2 sensing is normally achieved by measuring the pH change of an indicator in response to carbonic acid generated by the acidic CO_2 gas, many of the same reagents that are used for pH sensing are also used in absorption-based CO_2 sensing. Thymol blue immobilized in a sol−gel matrix has been used for gaseous CO_2 sensing,[152] while bromothymol blue in an ionic liquid matrix has been used for both gas-phase and dissolved CO_2 sensing.[153] Cresol red has been used in an optical fiber configuration in order to measure in vivo gastric CO_2.[154] Recent reviews by Mohr[155,156] reported the development of new indicator dyes for neutral and ionic analytes. Many of these use reversible covalent bond formation to detect analytes such as amines, cyanide, formaldehyde, nitrites, and peptides. Selective colorimetric optical probes based on pyrylium dyes have been developed recently for detection of aliphatic amines.[157,158] Novel, highly selective probes for formaldehyde detection have been developed by Suzuki et al.,[159] while a formaldehyde sensor, based on the reagent 4-amino dydrazine-5-mercapto-1,2,4-triazole, has been reported recently.[160] A highly selective colorimetric Hg^{2+} sensor, which uses a squaraine reporter dye, has been reported.[161] This highly toxic heavy-metal ion has also been detected optically by immobilizing dithizone on a triacetylcellulose membrane.[162] Squaraine derivatives have also been used for colorimetric detection of cyanide ions.[163] A fluoride-selective sensor based on the complexation of fluoride ion with an aluminum octaethylporphyrin ionophore dye has been reported.[164] The sensor exploits the fact that aluminum(III) forms very stable complexes with fluoride in aqueous solutions. A breath sensor for acetone measurement, which detects the colored product that is formed when acetone reacts with alkaline salicylaldehyde, has been reported by Teshima et al.[165]

4.2.2. Reagents for Luminescence Sensing

Analytes such as pH, CO_2, ammonia, O_2, and many cations and anions can be measured using luminescent probes. Luminescence is intrinsically more sensitive than absorption as a sensing technique, so, for many applications, luminescence-based sensing offers higher sensitivity than absorption sensors.

As in the case of absorption-based sensors, the principle of luminescence measurement of pH, CO_2, and ammonia relies on the change in luminescence of a pH indicator. For these analytes, the literature is dominated by two pH-dependent luminescent probes, namely, fluorescein and 8-hydroxypyrene-1,3,6-trisulfonic acid (HPTS). Both dyes absorb at convenient LED-emission wavelengths in the blue, while emission occurs just above 500 nm. Fluorescein has been used recently in an optical fiber imaging sensor based on drop-on-demand inkjet printing.[166] Fluorescein-related dyes have been used in order to facilitate covalent immobilization to the sensor matrix to eliminate dye leaching. For example, pH sensing has been realized using a fluoresceinamine isomer II complex that was covalently bound to a sol−gel matrix.[167] Ratiometric sensing is a self-referencing technique where either an analyte-insensitive excitation or a luminescence band of the dye is ratioed with the analyte-dependent band. Excitation ratiometric sensing has been achieved using methacryloyl-modified HPTS that facilitates covalent bonding to a polymer matrix and has a sensing range of pH 6−9.[168]

Ratiometric pH sensing has also been demonstrated using mercurochrome, another fluorescein-related dye, in a sol−gel matrix.[169] A newly synthesized boron−dipyrromethene derivative has been used in a single-excitation dual-emission ratiometric scheme to measure pH in human gastric juices.[170] Naphthalimides have also been investigated as luminescent probes,[171,172] while a pH sensor using covalently immobilized piperazinyl-1,8-napthalimide has been published recently.[173] Luminescent transition-metal complexes have larger Stokes shifts and longer lifetimes than, for example, fluorescein or HPTS. This allows more flexibility in excitation/detection optoelectronics as well as enabling lifetime-based sensing schemes. pH sensing has been demonstrated recently using a range of ruthenium and rhenium complexes based on the pH-sensitive ligand 5-carboxyl-1,10-phenanthroline.[174] In this work, the complexes have been tailored for maximum dynamic range.

Aminofluorescein has been used for optical ammonia sensing where an enhancement has been achieved compared to fluorescein-based sensing due to the reaction of the ammonia with the amine group on the fluorescent dye.[175] Ruthenium(II) tris(4,7-dephenyl-1,10-phenthroline) (Ru(dpp)$_3$) has been ion paired with the pH indicator bromophenol blue.[176] On exposure to ammonia, the increase in the deprotonated band of the pH indicator gives rise to energy transfer whereby the luminescence and lifetime of the Ru(dpp)$_3$ complex decreases.

In a novel, multianalyte approach, Nivens et al.[177] used HPTS to detect pH, CO_2, and NH_3 by designing multilayer sol−gel structures whereby, for CO_2 and NH_3 sensing, a hydrophobic outer layer is used to eliminate cross-reactivity to pH. HPTS has been widely used for CO_2 sensing, where, as above, the matrix has been tailored to prevent ingress of protons. HPTS is stable and water soluble, and the pK_a is ideal for CO_2 detection.[178] Lifetime-based sensing based on HPTS in polymer matrices has been reported.[179,180] A HPTS-based ratiometric sensor has been published recently for monitoring CO_2 in marine sediments.[181]

The luminophores used for optical oxygen sensing have been based mainly on organometallic complexes of ruthenium, in particular ruthenium polypyridyl complexes, and also metalloporphyrin complexes. However, a number of papers have reported on a range of polycyclic hydrocarbons (PAHs) that are efficiently quenched by oxygen.[182−184] Ruthenium polypyridyl complexes are characterized by high quantum efficiency and convenient absorption and emission maxima located in the visible spectrum with a large Stokes shift and relatively long lifetime (∼1 μs). These complexes are efficiently quenched in the presence of oxygen, giving rise to a decrease in both luminescence intensity and lifetime. The complex Ru(dpp)$_3$, referred to above in the context of pH sensing, has one of the longest unquenched lifetimes (∼5 μs) and been widely reported for oxygen-sensing applications, both in polymer and sol−gel matrices.[185−187] Porphyrin complexes have longer lifetimes (∼100 μs), emit at the red end of the visible spectrum, and are generally considered to have inferior photostability properties compared to ruthenium complexes. However, fluorinated porphyrins have been shown to be highly stable against photo-oxidation and photoreduction.[188] The most widely reported complexes for oxygen-sensing applications are the platinum and palladium octaethylporphyrin (PtOEP and PdOEP).[189,190] Platinum and palladium tetrakis(pentafluorophenyl)porphyrin (PtTFPP and PdTFPP) have also been reported.[191]

Ruthenium complexes have also been used for luminescence-based relative humidity sensing based on the quenching of a phenazine ligand by protons.[192−194]

There are extensive literature reports on the use of luminescent probes to measure anionic and cationic species as well as organic chemicals. Some of this work has been referenced in the recent review by Wolfbeis.[5] Probes used for chloride sensing include the chloride-quenchable lucigenin dye[14] and the halide-selective ionophore[9] mercuracarborand-3.[195] Aluminum(III) concentration has been measured using the dye 1,4-dihydroxyanthraquinone (quinizarin). Sensing is based on the highly fluorescent complex which is formed when Al^{3+} complexes with quinizarin.[196] Molecularly printed polymers (MIPs) have also been used where Al^{3+} is used as the template and 8-hydroxy-quinoline sulfonic acid is the luminescent tag which complexes to the Al^{3+} ion.[197] Badagu et al.[198] developed a range of cyanide-sensitive probes that are based on the binding of the cyanide ion to a boronic acid functional group. Both intensity and lifetime-based sensing have been demonstrated. Luminescence-based nitrate sensing has been achieved using the cationic potential-sensitive dye 4-(4-(dihexadecylamino)styryl-*N*-methylpyridinium iodide), which acts as an anion-exchange catalyst that extracts nitrate from aqueous solution to form a luminescent complex.[199]

4.2.3. Summary

Clearly, a comprehensive account of the large number and variety of absorption and luminescence probes reported in recent years is beyond the scope of this general review of optical chemical sensors. The most widely used reagents in areas such as pH and oxygen sensing have been highlighted. In the case of ion sensing, a selection of recently published work has been cited, which deals with some environmentally topical analytes such as chloride and aluminum ions.

4.3. Immobilization Matrices

4.3.1. Introduction

In most reagent-based optical sensors, the reagent is immobilized in a solid matrix usually in the form of a monolith or a thin film. The matrix serves to encapsulate the reagent such that it is accessible to the analyte while being impervious to leaching effects. In this section, two commonly used immobilization matrices will be described, namely, sol−gel and polymer materials, and a selection of work published in recent years will be reported for sol−gel and polymer-based absorption and luminescence sensors. Since the immobilization matrix very often influences the sensor response, a brief discussion of reagent−matrix interactions will be given.

4.3.2. Sol–Gel Matrices

The sol−gel process provides a relatively benign support matrix for the immobilization of analyte-sensitive reagents and dyes. The basic process involves the hydrolysis and polycondensation of the appropriate metal alkoxide solution to produce a porous glass matrix in which the reagent is encapsulated in a nanometer-scale cage-like structure and into which the analyte molecules can diffuse. The versatility of the process facilitates tailoring of the physicochemical properties of the material in order to optimize sensor performance. For example, key sol−gel process parameters such as sol pH, precursor type and concentration, water content, and curing temperature can be adjusted to produce materials of desired porosity and polarity.[200]

This tailorability was demonstrated for oxygen-sensitive films doped with the $Ru(dpp)_3$ complex and were fabricated using different ratios of tetraethoxyorthosilane (TEOS) and methyltriethoxysilane (MTEOS) precursors.[201] In a later study, the effect of the alkyl (R) chain length on the oxygen sensitivity was measured.[202] Monoalkoxysilanes of the form $(C_nH_{2n+1})-Si-(OR)_3$, where n ranges from 1 to 12, have been investigated and exhibit a linear oxygen response which increases up to C8 and then begins to decrease. The decrease in response at longer alkyl chain lengths was correlated with a decrease in oxygen diffusion coefficient in the matrix for these films. Very high oxygen sensitivities have been achieved using fluorinated sol−gel precursors. For example, oxygen sensitivities have been achieved using precursors such as 3,3,3-trifluoropropyl-trimethoxysilane (TFP−TMOS), which are ∼10 times greater than that achieved for MTEOS-based sensors.[203,204] This high sensitivity is attributed to the highly hydrophobic and nonpolar nature of the fluoro films. These materials also exhibit very high stability, with stabilities of up to 2 years being achieved for some formulations. Novel phenyl-substituted ORMOSILs were used as matrices for oxygen sensors based on both the $Ru(dpp)_3$ complex and a platinum(II)−octaethylporphyrin complex. A highly stable and sensitive oxygen response was obtained, and the films were sterilizable.[205]

As an alternative to physical entrapment, the analyte-sensitive dye can also be covalently bound to the sol−gel matrix. This can increase stability and eliminate dye-leaching effects in aqueous environments. Some examples have already been referred to in section 4.2.[167,168] A triethoxysilane-modified ruthenium tris(bipyridyl) ($Ru(bpy)_3^{2+}$) complex has been anchored to a range of polysiloxane matrices,[206] and an oxygen sensor based on the same complex has been recently reported where the complex was covalently grafted to 3-aminopropyltriethoxysilane.[207] The sensor exhibited no leaching and was used for dissolved oxygen measurement.

Sol−gel matrices have also been used for other analytes such as in pH and CO_2 sensing. As discussed in section 4.2, for pH sensing a hydrophilic matrix which allows ingress of protons is required, whereas for CO_2 sensing a more complex matrix is required which retains the water required for conversion of the gas to carbonic acid in the films but has sufficient hydrophobicity to be pH insensitive. These conditions have been achieved for both sol−gel and polymer matrices using an ion-pairing approach. This will be described in more detail in the next section as the majority of the literature on optical CO_2 sensors is based on polymer matrices. However, sol−gel-based optical CO_2 sensors for both gas and dissolved phase have been reported.[208,209,43]

Standard sol−gel materials have a nonordered, amorphous structure where diffusion of analytes can be limited by the random microporosity of the structure. Mesostructured porous films, on the other hand, have large open porosity, which can offer enhanced diffusion and accessibility for analytes. Mesoporous sol−gel sensor films have been realized via an evaporation-induced self-assembly (EISA) approach.[210,211] These films have a highly structured mesoporosity and excellent optical quality. The films are based on the surfactant cetyltrimethylammonium bromide (CTAB). The CTAB/Si and probe/Si ratio is optimized to give the required structure. A sensor to detect metallic cations was reported which was based on the chelating properties of dibenzoylmethane.[211] An oxygen sensor based on a mesostructured sol−gel silica matrix was also reported.[212] A ruthenium complex was grafted to the mesostructured network that was based on the precursor 3-(triethoxysilyl)-propyl isocyanate and CTAB as surfactant. It was established that the stability, homogeneity, and sensitivity of the matrix was superior to a nonmesoporous matrix where the dye was just physically entrapped.

A novel sol−gel-based sensor application has been reported whereby an optical fiber core is fabricated from reagent-doped porous sol−gel. Hence, the core acts as an active fiber core optical sensor (AFCOS). The fabrication and optical properties of the fiber were investigated, and a humidity sensor was constructed as proof of principle.[213] Oxygen sensing has been reported using calcined mesoporous silica spheres which have been postdoped with the $Ru(bpy)_3^{2+}$ complex.[214] The oxygen sensitivity was dependent on the pore morphology in the sphere, and the response times (2−4 min) were longer than for thin films and most likely related to the relatively large sphere diameter of 0.1−0.2 mm.

4.3.3. Polymer Matrices

Polymers have been widely used as support materials for a broad range of optical sensors. They have many desirable features and compare well with sol−gel matrices for most applications. While polymers may not be as photochemically stable or printable as sol−gels, some polymers are more suitable than sol−gels for high-temperature applications such as autoclavation. The most widely used materials include polystyrene (PS), polyvinyl chloride (PVC), polymethyl methacrylate (PMMA), polydimethyl siloxanes (PDMS), and polytetrafluoroethylenes (PTFE) and cellulose derivatives such as ethyl cellulose. As discussed in the previous section, hydrophobic matrices, for example, PMMA and PDMS, are selected as the optimum matrix for optical oxygen sensing,

while more hydrophilic matrices such as ethyl cellulose have been widely used for pH sensing. Much has been published on polymer-based oxygen sensors. Mills[215] carried out a comprehensive investigation of the effect of various polymers and plasticizers on the oxygen sensitivity for mainly ruthenium-complex-doped materials. It was clear from this work that the value of the oxygen diffusion coefficient in the material was the main contributing factor in the oxygen sensitivity. Of all materials studied, PDMS yielded the highest diffusion coefficient, which is associated with the opening and closing of void volumes in the polymer. It is to be noted that similarly high oxygen sensitivities were achieved using fluoro-sol−gel materials by Bukowski.[204] This has been attributed to the high O_2 diffusivity in fluorinated materials.[216] Polymer-based oxygen optrodes have been reported which withstand autoclavation. Polysulfone and polyetherimide materials were found to withstand steam sterilization at 135 °C.[217] It is thought that these polymers have a different water uptake compared with other materials such as polyvinylnaphthalene, which are destroyed under these conditions. The dissolved oxygen sensors based on these polymers, once calibrated, do not need recalibration in between sterilization cycles. Polysulfone was also used successfully to monitor cell viability by measuring the oxygen consumption.[218] A novel oxygen sensor membrane has been reported by Holmes-Smith et al.[219] where an electropolymerized diphenyl-di(4-aminophenyl)porphyrin (Pt-(II)DAPP) has been characterized and tested as an optical oxygen sensor. The sensitivity obtained was comparable to other Pt−porphyrin systems reported in the literature, but the main advantages of this sensor were the versatility of deposition via the electropolymerization technique as well as the lack of leaching as the porphyrin is part of the polymer.

Optical CO_2 sensors are generally based on the Severinghaus principle, which relies on conversion of the gas to carbonic acid. In the presence of bicarbonate, it has been shown that the partial pressure of CO_2 is directly related to the pH change of a colorimetric or luminescent pH indicator.[178] In solid optical CO_2 sensors, a phase-transfer agent such as tetraoctylammonium hydroxide (TOAOH), a quaternary ammonium hydroxide, is used to solubilize the pH indicator into a hydrophobic polymer which acts as a proton barrier and reduces cross-sensitivity to pH. This gives rise to formation of an ion pair which facilitates encapsulation of the dye in the gas-permeable polymer. The quaternary ammonium hydroxide is normally associated with sufficient water molecules to facilitate formation of carbonic acid.

A fiber optic microsensor based on ion-paired HPTS in an ethyl cellulose matrix has been reported for high-resolution pCO_2 monitoring in the marine environment.[220] A gas-permeable but ion-impermeable coating was used as a protective layer to eliminate interferences such as chloride and pH, and the limit of detection achieved was 60 ppb. A highly stable, autoclavable sensor, based on HPTS ion paired to cetyltrimethylamonium hydroxide (CTMAOH) in a two-component silicone film, has been investigated for use in biofermentation.[221] PDMS and vinyl-terminated dimethylsiloxane copolymers were used to make the sensor film using a three-step process. The sensor used ratiometric detection, was stable for several months and sterilizable, and had an LOD of 0.03% CO_2.

It has been observed that CO_2 sensors based on a quaternary ammonium hydroxide base can have a limited shelf life in ambient air due to the ingress of other acidic gases such as NO_x and SO_2, which cause irreversible protonation of the indicator. It has been suggested that this is due to a process called Hofmann degradation.[222] The feasibility of replacing the quaternary base with a neutral phosphazene base which would not be susceptible to degradation has been investigated by Schroder et al.[223] Ethyl cellulose was the polymer used, and *p*-xylenol blue was the colorimetric pH indicator. The CO_2 response of the new phosphazene base system was generally comparable to that of the quaternary base system. However, the new base could only be used in dissolved phase due to its volatility, and the sensor film exhibited cross-sensitivity to relative humidity.

Molecularly imprinted polymers (MIPs) are being increasingly used as sensor supports. MIPs are synthesized by copolymerizing functional and cross-linking monomers in the presence of a target analyte molecule which acts as a template or imprint. When the template molecule is removed, the resulting cavity has a "memory" of the target analyte which imparts a high degree of selectivity to the MIP material.[224] A polyurethane-based MIP sensor imprinted with anthracene was reported where a theoretical model of the sensor response was developed in order to provide an optimization strategy for sensor design.[225] MIP sensors for detection of PAHs have been synthesized where the selectivity was tuned using different polystyrenes. Selectivity was tuned down to differences in size as little as one methyl group.[226] Because of their selectivity, MIPs are now being developed for biosensor applications where antibodies and enzymes are used as templates. Reviews dealing with MIPs for biosensor and other applications include those by Al-Kindy et al.[227] and Kindschy et al.[228] Apart from their high degree of selectivity, MIP sensor materials are generally very robust, stable, and resistant to interferences such as pH and humidity.[225]

4.3.4. Interaction of Reagent and Support Matrix

In order to be efficiently encapsulated in the support matrix, the reagent must be soluble in the support material. To enhance solubility, an ion-pairing approach can be used as discussed above for CO_2-based sensing. In the case of sol−gel matrices, for example, in order to encapsulate oxygen-sensitive ruthenium complexes, the counterion and sol−gel solvent can be chosen to facilitate homogeneous distribution of the dye in the matrix. In the case of optical oxygen sensors, the linearity of the Stern−Volmer (SV) sensitivity plot is strongly dependent on the matrix. For most sol−gel and polymer materials, a downward curved SV plot is obtained due to the inhomogeneous nature of the amorphous matrix where each dye molecule experiences a slightly different microenvironment. However, linear SV plots have been obtained, for example, where the indicator dye is soluble in the matrix and homogeneously entrapped in a defined polymer microdomain.[229] Linear SV plots have also been obtained for sol−gel materials which use precursors with long alkyl chain groups.[202,204]

The optical properties of some reagents are very sensitive to the environment; thus, often these reagents will experience spectroscopic shifts when encapsulated in a solid matrix. Of all the oxygen-sensitive ruthenium complexes, the spectroscopic properties of $Ru(dpp)_3$ are relatively insensitive to the sensor matrix.[230] In fact, these complexes exhibit enhanced fluorescence and longer decay times in solid matrices compared to in solution due to the reduction in nonradiative decay pathways. A substantial improvement in

selectivity and sensitivity has been observed in the case of the metal-ion indicator pyrocatechol violet (PV) when encapsulated in a plasticized PVC membrane. A shift in the working wavelength was accompanied by enhanced sensitivity to Cu(II) ions. This is possibly due to a reduction in the complexation ability of the dye and the different permeability selectivity imparted by the PVC matrix compared to solution behavior.[231]

Many optical sensor reagents photodegrade under conditions of high-intensity illumination, and in many cases the matrix has on influence on the degree of photodegradation. In general, reagents entrapped in rigid supports exhibit increased photostability due to reduced ligand photodegradation compared to a solution environment.[232] It has been shown that reagents encapsulated in sol−gel matrices have higher photostability than in polymer matrices. It has been suggested that the more organic polymer environment provides less stability than the more inorganic sol−gel matrix. In the case of oxygen-sensitive dyes, as mentioned in section 4.1, transition-metal complexes, for example, the ruthenium complexes, have higher stability than porphyrin complexes in general, but fluorinated porphyrin complexes exhibit high photostability.[182] It has been established that, for oxygen sensors, singlet oxygen, which is a byproduct of the quenching process, causes ligand dissociation in oxygen-sensitive dyes.[233] This degradation process is minimized in fluorinated matrices, either polymer or sol−gel based, which provide highly stable environments due to the high electronegativity of the C−F bond.[182,203] In general, the behavior of the reagent can be dependent on the matrix as well as the analyte concentration.

4.4. Recent Developments in Absorption-Based Sensors

Reagent-mediated absorption or colorimetric sensing has already been dealt with in section 4.2 on reagents, where numerous examples were given of colorimetric sensing for a wide range of analytes including pH, ammonia, and some ion-sensing applications. This brief section will highlight some recent examples of colorimetric sensors including some novel sensing techniques.

A generic sensing platform has been reported which is based on a flexible fused silica capillary.[234] The inner surface of a flexible light-guiding capillary was coated with a reagent-doped film, either polymer or sol−gel, to produce a long-path evanescent-wave-based sensor. The authors suggest that the flexibility and robustness of the fused silica capillary and the increased sensitivity provided by the increased length offer advantages over conventional optical fiber-based sensors as well as over previously reported capillary-based sensors. Sensing has been demonstrated for ammonia, toluene, and Cu(II) using this system. Cu(II) was detected down to 2.5 ppb, while ammonia was detected down to 15 ppm in the as-yet unoptimized system.

A dynamic technique for measuring pH over a very wide range has been reported, where the limited measurable pH range of the indicator in normal steady state measurements has been overcome using a flow system and optimizing the diffusion of the analyte in the sensor membrane.[235] In this work, the pH indicator was immobilized in a triacetyl cellulose membrane. The optical response to pH was measured before equilibrium was reached. At a fixed time before equilibrium, a linear plot is obtained for absorbance versus pH at any flow rate. The time and flow rate are optimized for maximum linear dynamic range. pH was determined over a range of up to 11 pH units.

A combination of a colorimetric and fluorometric reagent has been used to measure CO_2 where the luminescence change of a tetraphenylporphyrin dye due to the CO_2-dependent change in absorbance of a co-immoblized α-naphtholphthalein dye was measured.[236] The technique relied on the overlapping absorption and luminescence of the colorimetric and fluorometric reagents, respectively, and the fluorophore which was insensitive to CO_2 acted as an internal reference. The sensor operated in both gas and dissolved phase, was immune to photobleaching, and exhibited short response times of <6 s in the gas phase. The same authors used a thymol blue−europium complex combination for gas-phase CO_2 sensing.[237]

Mesoporous sensor matrices have already been discussed in section 4.3. A fiber-based colorimetric pH sensor based on bromothymol blue in a mesostructured silica film has been reported.[238] The sensor responds over the pH range 2−5. Dye leaching is overcome by tailoring the mesopore dimensions to entrap the dye molecule, while the hydrophilic nature of the pore wall allows adsorption of the dye via hydrogen bonds.

A CO_2 sensor based on ion-paired bromothymol blue, which has been dissolved in an ionic liquid matrix, has been reported.[239] The solubility of CO_2 in water- miscible ionic liquids, such as 1-methyl-3-butylimidazolium tetrafluoroborate used in this work, is 10−20 times that observed in conventional solvent and polymer matrices. Sensing of CO_2 was demonstrated both in gas and dissolved phase. However, regeneration of the reagent phase using nitrogen was necessary, and pH interference studies have not been reported in this preliminary report. The same authors reported a luminescence-based CO_2 sensor based on HPTS dissolved in similar ionic liquid matrices.[240]

4.5. Recent Advances in Luminescence-Based Sensors

4.5.1. Introduction

Reagent-based luminescence sensing can be based on monitoring the intensity of the luminescence, often using a ratiometric approach as mentioned in section 4.2.2, or the reagent lifetime can be monitored via a lifetime-dependent phase measurement for example. Simply monitoring the intensity, in the absence of an analyte-independent reference, can give rise to drift and instability due to light source and detector drift, changes in optical path, and drift due to degradation or leaching of the dye. These problems can be overcome to a large extent by employing ratiometric sensing which, as explained in section 4.2.2, involves taking the ratio between an analyte-dependent luminescence or excitation band and a second band which is analyte independent. Referenced sensing can also be achieved using techniques such as phase fluorometry and dual-luminophore referencing (DLR), which will be explored in more detail in section 4.5.3. This section will be divided into a review of recently reported intensity-based sensing and a discussion of lifetime-based sensing, including some recent examples.

4.5.2. Intensity-Based Sensing

Fiber optic oxygen sensors based on two different Pt(II) complexes encapsulated in a fluorinated sol−gel matrix have been reported.[241] A composite matrix of *n*-propyltrimethoxy-

silane and 3,3,3-trifluoropropyltrimethoxysilane was doped with either platinum tetrakis(pentafluorophenyl)porphine (PtTFPP) or platinum octaethylporphine (PtOEP). The higher oxygen sensitivity of metalloporphyrin complexes compared to ruthenium complexes has already been discussed in section 4.3, as also has the stability and enhanced oxygen permeability offered by fluoro sol−gel matrices. Both sensor materials demonstrated very high oxygen sensitivity, linear SV response, and short response times of ~5 s.

The disadvantages of intensity sensing have been addressed by the work of Tang et al.,[242] where tailored sol−gel sensor arrays were employed to yield improved accuracy and precision in O_2 detection with the use of artificial neural networks (ANN). Pin-printed arrays, where each element has a different O_2 response profile, are produced. The tailored oxygen response is achieved by co-doping the sol−gel with different ratios of two ruthenium complexes which have very different oxygen sensitivities. The ANN was "trained" to identify the CCD images from the array. Overall, a 5−10-fold improvement in accuracy and precision compared to a single-element sensor was achieved for quantifying O_2 in unknown samples.

Transparent nanostructured metal oxide oxygen sensor matrices were fabricated by embedding oxides such as aluminum oxide, silicon oxide, and zirconium oxide in PVA.[243] Organometallic complexes of ruthenium or iridium were used as oxygen-sensitive dyes, which were incorporated in the nanostructured matrix. SV constants for these matrices were ~100 times larger than for the same dyes incorporated in conventional polymer matrices. Furthermore, the materials were sterilizable by autoclavation and γ radiation, exhibited response times of <1 s, and were stable for up to 9 months. The superior oxygen sensor performance was attributed mainly to the nanoporosity and high total pore volume of the nanostructured matrices.

The majority of both colorimetric and fluorometric pH indicators reported in the literature and in this review operate in the acidic or neutral pH range. Recently, luminescent pH indicators based on Schiff bases have been developed which respond in the pH range 7−12.[244] The indicators chlorophenyliminopropenylaniline (CPIPA) and nitrophenyliminopropenylaniline (NPIPA), with pK_a values of 10.30 and 8.80, respectively, have been immobilized in PVC. Photostability was superior to fluorescein for both dyes, and CPIPA in PVC matrix exhibited an enhanced quantum yield and reversible pH response over the basic pH range. Both dyes have convenient absorption and emission bands in the visible spectrum.

A Li^+ sensor for clinical applications, which is based on a polymer derivative of a novel lithium fluoroionophore, has been reported.[245] The fluoroionophore is based on a tetramethyl blocking subunit of a 14-crown-4 as a Li^+-selective binding site and 4-methylcoumarin as a luminophore. Ratiometric detection is enabled by the quenching of the main emission band by Li^+ and the simultaneous appearance of a blue-shifted shoulder. The sensor exhibits good reversibility and immunity from interference for pH and the major biological interfering cations, K^+, Ca^{2+}, and Mg^{2+}.

Highly selective K^+ sensing has been demonstrated using a fluoroionophore based on aza-18-crown-6 as K^+ chelator and the fluorophore BODIPY (from Molecular Probes Inc.). The cavity size of the crown ether is chosen to be selective for K^+ and discriminate against Na^+ ions. By using novel substitution reactions of the BODIPY complex, the system was tailored such that the emission band shifts from ~529 to 504 nm in the presence of K^+, which facilitates ratiometric optical detection.[246]

Advances in array-based biosensing have been summarized in a recent review by Ligler.[247] The main focus of this review is development of a portable, multianalyte luminescence-based array biosensor by the Naval Research Laboratories (NRL). The device uses planar waveguide optical coupling and PDMS microfluidics to allow simultaneous detection and quantification of multiple target analytes and multiple samples.[248] The array-based biosensor has been used for antibody detection, for example, to detect food borne contaminants such as staphylococcal enterotoxin B and other toxins[249] and the toxin deoxynivalenol, which is a common food contaminant. LODs of <1 ng/mL were achieved in each case. The system has also been used to detect bioterrorism agents such as anthrax.[250]

4.5.3. Lifetime-Based Sensing

A primary disadvantage associated with the use of fluorescence intensity detection techniques is the susceptibility of sensors based on such techniques to signal fluctuations caused by changes in excitation source intensity, photobleaching of the fluorescent indicator complex, or changes in the concentration of the indicator within the sensing environment (due, for example, to leaching). A more robust fluorescence detection strategy involves measuring analyte-induced changes in the lifetime of the indicator compound, as this parameter is unaffected by the factors mentioned above.

Sensors based on detection of fluorescence lifetime may be broadly divided into those that directly measure the lifetime and those that employ phase measurement techniques to indirectly monitor the lifetime. Systems that employ direct lifetime measurement techniques typically include a pulsed laser source and gated, or delayed, detection with a suitable photodetector, e.g., a photon-counting photomultiplier tube or intensified CCD camera. Such systems have been applied to detection of water in organic solvents,[192] pH,[251−253] and oxygen[204,254] in recent years.

However, the cost and complexity of systems capable of direct fluorescence lifetime measurements render them less attractive for development of low-cost, mass-producible systems. This has been an important driver in optical chemical sensor research in recent years, and while some efforts have been made to develop low-cost lifetime measurement systems,[255] more effort has been applied to development of phase measurement instrumentation, which is well suited to development of low-cost sensor platforms. Perhaps the most common example of a luminescence-based sensor that utilizes phase measurement techniques is that of a phase fluorometric oxygen sensor.[10,39,40,256−260] The concept of phase fluorometry is illustrated in Figure 9.

The excitation source is modulated at a particular frequency, and the emitted fluorescence is similarly modulated but phase shifted relative to the excitation signal. Phase measurement electronics are used to measure this phase shift, which is related to the luminescence lifetime by eq 1

$$\tan \phi = 2\pi f\tau \quad (1)$$

where ϕ is the measured phase angle, f is the modulation frequency, and τ is the lifetime of the luminescent complex. This measurement concept can be implemented using low-cost phase detection electronics in conjunction with LED

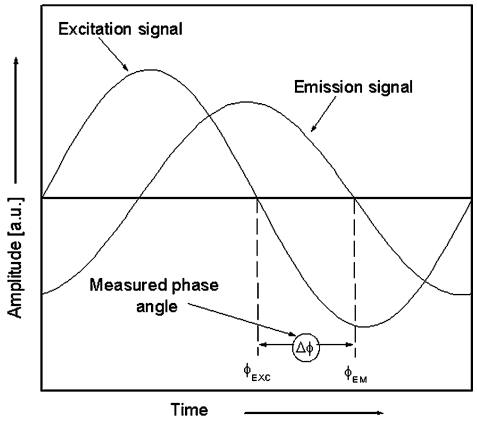

Figure 9. Principle of phase fluorometry.

sources and photodiode detectors, making it an extremely attractive candidate for development of commercial oxygen sensors by companies such as PreSens Precision Sensing GmbH [www.presens.de], YSI environmental [www.ysi-.com], Gas Sensor Solutions [www.gss.ie], Ocean Optics [www.oceanoptics.com], and Interlab [www.interlab.es]. The technique has also recently been applied to development of optical humidity sensors.[193,194]

An important element in development of a phase fluorometric sensor is the use of an indicator complex that is sufficiently long lived so as to be accessible to the modulation frequency range provided by the low-cost sensor electronics, which typically requires that the lifetime be at least in the single microsecond regime. In the case of phase fluorometric oxygen sensors, indicators based on ruthenium or porphyrin dye complexes adequately fulfill this role, but for analytes such as carbon dioxide, pH, or chloride, the fluorescent indicators employed are not sufficiently long lived to be directly accessible to phase fluorometric detection strategies. In response to this, a number of strategies have been developed with the goal of rendering the intrinsically intensity-based measurements required for detection of such analytes compatible with phase fluorometry instrumentation. This would then allow for development of multianalyte sensor technology requiring only a single instrumentation platform. Fluorescence resonance energy transfer (FRET) has been exploited in the past to bring intensity measurements into the phase domain.[208,261] However, the most predominant example of a technique that fulfils this goal is dual-lifetime referencing (DLR), also referred to as dual-luminophore referencing, which was first reported by Huber et al. in 2000[262] and has been applied to detection of analytes such as CO_2,[195, 20943, 263] pH,[264,265] nitrate,[266] copper(II) ions,[267] and chloride.[199] As the name suggests, the DLR technique makes use of two luminescent indicators that are typically co-immobilized within a solid matrix. One of the indicators is analyte sensitive and possesses a short luminescence lifetime; the other is analyte insensitive and long lived. Changes in the fluorescence intensity ratio of the two compounds are reflected as changes in the measured phase angle (see Figure 10), thereby facilitating the use of phase detection instrumentation in the realization of any sensor that exploits this technique.

Additionally, Borisov et al. recently reported the use of a modified DLR (m-DLR) technique that facilitates the simultaneous detection of two analytes.[268] A related technique is that of gated phase-modulation (GPM) fluorometry,[269] which is similar to DLR in that it makes use of two

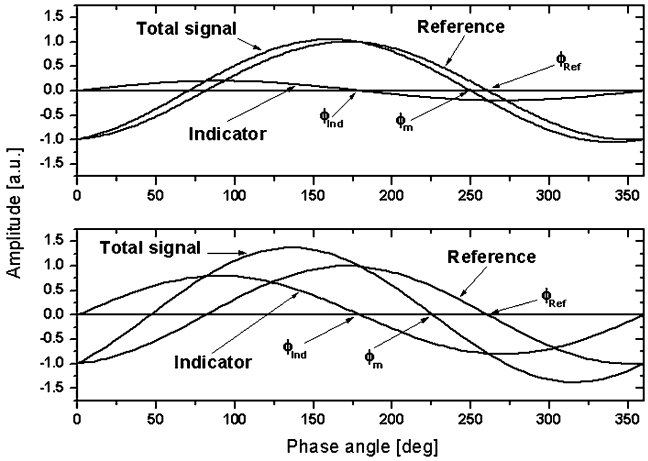

Figure 10. Principle of dual-lifetime referencing (DLR). Changes in the amplitude of the indicator signal that are caused by changes in analyte concentration result in a modification of the measured phase angle, ϕ_m. This is shown above for two different indicator signal amplitudes.

luminophores with long and short lifetimes, but unlike DLR, square-wave modulation is employed in conjunction with gated detection in order to develop sensors for analytes such as pH.

5. Key Trends and Future Perspectives

While the basic sensor transduction principles employed in optical chemical sensors are now well established and remain largely unchanged over the years, there have been significant recent advances in both the design of sensor platforms and strategies for performance enhancement. These developments, which are likely to drive future trends in the research and development of optical chemical sensors, include advances in nanomaterials, microfluidics, wireless networks, as well as optical materials and components.

As in many other areas of scientific research, many developments in optical chemical sensors (OCS) are to be found at the micro−nano interface. The massive investment in nanotechnology across the world is leading to new materials and structures, the unique properties of which can have significant implications for the design and implementation of OCS. For example, the area of plasmonics, which is based primarily on the novel optical properties associated with localized surface plasmon resonance on metal nanoparticles and nanostructured surfaces, is attracting considerable research attention with conferences and a new journal dedicated to the topic. The key implications of plasmonics for optical chemical sensing are in nanoscale sensors (e.g., refractometric) and enhancements of spectroscopic sensors. For example, surface-enhanced Raman scattering (SERS) is an area that has been the subject of intensive research over a relatively short time frame for development of ultrasensitive diagnostic devices. A number of novel geometries/platforms based on metal nanoparticles/nanostructures have been developed recently,[134,135] and these have resulted in improved sensitivity and sensor stability. Research in this area is likely to accelerate further in coming years. Similarly, the area of metal-enhanced fluorescence[270−273] (MEF) is attracting considerable attention and likely to play a key role in sensitivity enhancement strategies over the coming years as the underlying principles of this phenomenon become better understood. Another area where the impact of nanotechnology is likely to be seen is in the use of nanowires; the use

of subwavelength nanowires as evanescent wave-based optical sensors was recently reported.[274]

Nanomaterials must be supported on a suitable platform which must often provide additional functionalities such as sample delivery and signal collection. Such platforms typically employ features in micrometer dimensions, and this highlights the increasingly important role that microsystems and microfluidics will play in the future development of OCS. More generally, OCS employing microfluidics (lab-on-a-chip; micro-total analysis systems (μTAS); Bio-MEMS) will see significant growth especially in the context of (bio)-sensor arrays and the need for miniaturized systems. It is important to note here that such microfluidic systems may also enable the use of chemical sensors based on renewable reagents (using irreversible indicators which would otherwise not be suitable for sensors) by virtue of the low volumes involved. Such miniaturized systems are also critical in the field of wireless sensor networks, which is the subject of a separate review in this issue. This area is likely to have a profound impact on our society as a whole, potentially providing real-time information on environmental and health-related parameters in a spatially distributed context. Another area where developments in microfluidics are likely to see major application is in the fabrication of low-cost diagnostic platforms for widespread use, e.g., in the home but more significantly for application in low resource environments (global diagnostics).

Advances in optical materials and platforms are likely to play an important role in future developments of OCS. For example, refractometric sensor platforms based on geometries such as microsphere[275,276] or microring[277] resonators and 2D photonic crystals[278] show promise for development of compact, array-based chemical sensors, while a number of groups have emphasized and demonstrated the importance of integration of all aspects of the sensor platform (i.e., source, sample, detector) onto a single chip using, for example, CMOS technology.[279−281]

The use of quantum dots for optical sensing is a rapidly developing area. In particular, quantum dots are increasingly being used as high-brightness fluorescent labels in optical biosensing. These nanoscale colloidal semiconductors have many advantages over conventional dye labels, for example, very high quantum efficiencies, narrow, tunable emission bands, and enhanced stability. It is likely that ongoing improvements in synthesis and functionalization of quantum dots will lead to a new generation of luminescence-based optical sensors.[282−285]

Another recent innovation in fluorescence-based sensor research is the exploitation of fluorescence emission anisotropy in the design of highly efficient, ultrasensitive sensor platforms based on a range of optical elements and platforms.[285−288] Such platforms can enhance sensitivity by a factor of up to 100 and will have significant implications for development of efficient, low-cost diagnostic platforms.

In conclusion, the field of OCS, which is based on solid fundamental principles, has an exciting future as the need for rapid supply of measurement information increases and the convergence of disparate technologies provides significant opportunities for performance enhancement.

6. References

(1) Wolfbeis, O. S. *Fibre Optic Chemical Sensors and Biosensors*; CRC Press: Boca Raton, 1991; Vols. 1 and 2.
(2) Orellana, G.; Moreno-Bondi, M. C. *Frontiers in Chemical Sensors*: *Novel Principles and Techniques*; Springer: New York, 2005.
(3) Baldini, F.; Chester, A. N.; Homola, J.; Martellucci, S. *Optical Chemical Sensors*; NATO Science Series 224; Springer: New York, 2006.
(4) *Optical Sensors − Industrial, Environmental and Diagnostic Applications*; Edited by R. Narayanaswamy and O. S. Wolfbeis, Springer Series on Chemical Sensors and Biosensors (ed. O. S. Wolfbeis), Vol. 1, Springer, 2004.
(5) Wolfbeis, O. S. *Anal. Chem.* **2006**, *78*, 3859.
(6) Cammann, G. G.; Guilbault, E. A.; Hal, H.; Kellner, R.; Wolfbeis, O. S. *The Cambridge Definition of Chemical Sensors, Cambridge Workshop on Chemical Sensors and Biosensors*; Cambridge University Press: New York, 1996.
(7) Oberg, K. I.; Hodyss, R.; Beauchamp, J. L. *Sens. Actuators, B: Chem.* **2006**, *115*, 79.
(8) Alves, F. L.; Raimundo, I. M.; Gimenez, I. F.; Alves, O. L. *Sens. Actuators, B: Chem.* **2005**, *107*, 47.
(9) O'Neal, D. P.; Meledeo, M. A.; Davis, J. R.; Ibey, B. L.; Gant, V. A.; Pishko, M. V.; Cote, G. L. *IEEE Sens. J.* **2004**, *4*, 728.
(10) Valledor, M.; Carlos Campo, J.; Sanchez-Barragan, I.; Carlos Viera, J.; Costa-Fernandez, J. M.; Sanz-Medel, A. *Sens. Actuators, B: Chem.* **2006**, *117*, 266.
(11) Chen, L. X.; Niu, C. G.; Xie, Z. M.; Long, Y. Q.; Song, X. R. *Anal. Sci.* **2006**, *22*, 977.
(12) Wang, X.; Zeng, H. L.; Zhao, L. X.; Lin, J. M. *Talanta* **2006**, *70*, 160.
(13) Vasylevska, G. S.; Borisov, S. M.; Krause, C.; Wolfbeis, O. S. *Chem. Mater.* **2006**, *18*, 4609.
(14) Huber, C.; Klimant, I.; Krause, C.; Wolfbeis, O. S. *Anal. Chem.* **2001**, *73*, 2097.
(15) Alfeeli, B.; Pickrell, G.; Wang, A. B. *Sensors* **2006**, *6*, 1308.
(16) Eom, I. Y.; Dasgupta, P. K. *Talanta* **2006**, *69*, 906.
(17) Tung, Y. C.; Zhang, M.; Lin, C. T.; Kurabayashi, K.; Skerlos, S. J. *Sens. Actuators, B: Chem.* **2004**, *98*, 356.
(18) Camou, S.; Fujita, H.; Fujii, T. *Lab Chip* **2003**, *3*, 40.
(19) Yang, B. C.; Tian, H. Z.; Xu, J.; Guan, Y. F. *Talanta* **2006**, *69*, 996.
(20) Hofmann, O.; Wang, X. H.; deMello, J. C.; Bradley, D. D. C.; deMello, A. J. *Lab Chip* **2005**, *5*, 863.
(21) Chabinyc, M. L.; Chiu, D. T.; McDonald, J. C.; Stroock, A. D.; Christian, J. F.; Karger, A. M.; Whitesides, G. M. *Anal. Chem.* **2001**, *73*, 4491.
(22) Ahmad, M.; Chang, K. P.; King, T. A.; Hench, L. L. *Sens. Actuators, A: Phys.* **2005**, *119*, 84.
(23) Park, E. J.; Reid, K. R.; Tang, W.; Kennedy, R. T.; Kopelman, R. *J. Mater. Chem.* **2005**, *15*, 2913.
(24) Preejith, P. V.; Lim, C. S.; Chia, T. F. *Meas. Sci. Technol.* **2006**, *17*, 3255.
(25) Bowden, M.; Song, L. N.; Walt, D. R. *Anal. Chem.* **2005**, *77*, 5583.
(26) Ahn, S.; Kulis, D. M.; Erdner, D. L.; Anderson, D. M.; Walt, D. R. *Appl. Environ. Microbiol.* **2006**, *72*, 5742.
(27) Moreno, J.; Arregui, F. J.; Matias, I. R. *Sens. Actuators, B: Chem.* **2005**, *105*, 419.
(28) Gupta, B. D.; Sharma, N. K. *Sens. Actuators, B: Chem.* **2002**, *82*, 89.
(29) James, S. W.; Tatam, R. P. *J. Opt. A: Pure Appl. Opt.* **2006**, *8*, S430.
(30) King, D.; Lyons, W. B.; Flanagan, C.; Lewis, E. *Meas. Sci. Technol.* **2004**, *15*, 1560.
(31) Sang, X. Z.; Yu, C. X.; Yan, B. B.; Ma, J. X.; Meng, Z. F.; Mayteevarunyoo, T.; Lu, N. G. *Chin. Phys. Lett.* **2006**, *23*, 3202.
(32) Falciai, R.; Mignani, A. G.; Vannini, A. *Sens. Actuators, B: Chem.* **2001**, *74*, 74.
(33) DeLisa, M. P.; Zhang, Z.; Shiloach, M.; Pilevar, S.; Davis, C. C.; Sirkis, J. S.; Bentley, W. E. *Anal. Chem.* **2000**, *72*, 2895.
(34) Pisco, M.; Consales, M.; Campopiano, S.; Viter, R.; Smyntyna, V.; Giordano, M.; Cusano, A. *J. Lightwave Technol.* **2006**, *24*, 5000.
(35) Liu, N.; Hui, J.; Sun, C. Q.; Dong, J. H.; Zhang, L. Z.; Xiao, H. *Sensors* **2006**, *6*, 835.
(36) Kang, Y.; Ruan, H.; Wang, Y.; Arregui, F. J.; Matias, I. R.; Claus, R. O. *Meas. Sci. Technol.* **2006**, *17*, 1207.
(37) Benounis, M.; Jaffrezic-Renault, N.; Dutasta, J. P.; Cherif, K.; Abdelghani, A. *Sens. Actuators, B: Chem.* **2005**, *107*, 32.
(38) Jung, Y.; Kim, S.; Lee, D.; Oh, K. *Meas. Sci. Technol.* **2006**, *17*, 1129.
(39) Burke, C. S.; McGaughey, O.; Sabattie, J. M.; Barry, H.; McEvoy, A. K.; McDonagh, C.; MacCraith, B. D. *Analyst* **2005**, *130*, 41.
(40) McDonagh, C.; Kolle, C.; McEvoy, A. K.; Dowling, D. L.; Cafolla, A. A.; Cullen, S. J.; MacCraith, B. D. *Sens. Actuators, B: Chem.* **2001**, *74*, 124.
(41) Malins, C.; Niggemann, M.; MacCraith, B. D. *Meas. Sci. Technol.* **2000**, *11*, 1105.
(42) Chang-Yen, D. A.; Gale, B. K. *Lab Chip* **2003**, *3*, 297.

(43) Burke, C. S.; Markey, A.; Nooney, R. I.; Byrne, P.; McDonagh, C. *Sens. Actuators, B: Chem*. **2006**, *119*, 288.
(44) Huang, S. H.; Tseng, F. G. *J. Micromech. Microeng.* **2005**, *15*, 2235.
(45) Rowe-Taitt, C. A.; Golden, J. P.; Feldstein, M. J.; Cras, J. J.; Hoffman, K. E.; Ligler, F. S. *Biosens. Bioelectron.* **2000**, *14*, 785.
(46) Duveneck, G. L.; Abel, A. P.; Bopp, M. A.; Kresbach, G. M.; Ehrat, M. *Anal. Chim. Acta* **2002**, *469*, 49.
(47) Chronis, N.; Lee, L. P. *Lab Chip* **2004**, *4*, 125.
(48) Gouin, J. F.; Doyle, A.; MacCraith, B. D. *Electron. Lett.* **1998**, *34*, 1685.
(49) Zourob, M.; Mohr, S.; Fielden, P. R.; Goddard, N. J. *Sensors Actuators, B: Chem.* **2003**, *94*, 304.
(50) Malins, C.; Doyle, A.; MacCraith, B. D.; Kvasnik, F.; Landl, M.; Simon, P.; Kalvoda, L.; Lukas, R.; Pufler, K.; Babusik, I. *J. Environ. Monit.* **1999**, *1*, 417.
(51) Lavers, C. R.; Itoh, K.; Wu, S. C.; Murabayashi, M.; Mauchline, I.; Stewart, G.; Stout, T. *Sens. Actuators, B: Chem.* **2000**, *69*, 85.
(52) Yang, L.; Saavedra, S. S. *Anal. Chem.* **1995**, *67*, 1307.
(53) Yang, L.; Saavedra, S. S.; Armstrong, N. R. *Anal. Chem.* **1996**, *68*, 1834.
(54) Skrdla, P. J.; Armstrong, N. R.; Saavedra, S. S. *Anal. Chim. Acta* **2002**, *455*, 49.
(55) Puyol, M.; del Valle, M.; Garces, I.; Villuendas, F.; Dominguez, C.; Alonso, J. *Anal. Chem.* **1999**, *71*, 5037.
(56) Puyol, M.; Salinas, I.; Garces, I.; Villuendas, F.; Llobera, A.; Dominguez, C.; Alonso, J. *Anal. Chem.* **2002**, *74*, 3354.
(57) Hisamoto, H.; Kim, K.; Manabe, Y.; Sasaki, K.; Minamitani, H.; Suzuki, K. *Anal. Chim. Acta* **1997**, *342*, 31.
(58) Qi, Z. M.; Yimit, A.; Itoh, K.; Murabayashi, M.; Matsuda, N.; Takatsu, A.; Kato, K. *Opt. Lett.* **2001**, *26*, 629.
(59) Burke, C. S.; Polerecky, L.; MacCraith, B. D. *Meas. Sci. Technol.* **2004**, *15*, 1140.
(60) Lambeck, P. V. *Meas. Sci. Technol.* **2006**, *17*, R93.
(61) Gauglitz, G. *Anal. Bioanal. Chem.* **2005**, *381*, 141.
(62) Hua, P.; Luff, B. J.; Quigley, G. R.; Wilkinson, J. S.; Kawaguchi, K. *Sens. Actuators, B: Chem.* **2002**, *87*, 250.
(63) Prieto, F.; Sepulveda, B.; Calle, A.; Llobera, A.; Dominguez, C.; Abad, A.; Montoya, A.; Lechuga, L. M. *Nanotechnology* **2003**, *14*, 907.
(64) Qi, Z. M.; Matsuda, N.; Itoh, K.; Murabayashi, M.; Lavers, C. R. *Sens. Actuators, B: Chem.* **2002**, *81*, 254.
(65) Sepúlveda, B.; Río, J. S. d.; Moreno, M.; Blanco, F. J.; Mayora, K.; Domínguez, C.; Lechuga, L. M. *J. Opt. A: Pure Appl. Opt.* **2006**, *8*, S561.
(66) Esinenco, D.; Psoma, S. D.; Kusko, M.; Schneider, A.; Muller, R. *Rev. Adv. Mater. Sci.* **2005**, *10*, 295.
(67) Heideman, R. G.; Lambeck, P. V. *Sens. Actuators, B: Chem*. **1999**, *61*, 100.
(68) Ymeti, A.; Greve, J.; Lambeck, P. V.; Wink, T.; van Hovell, S. W. F. M.; Beumer, T. A. M.; Wijn, R. R.; Heideman, R. G.; Subramaniam, V.; Kanger, J. S. *Nano Lett.* **2007**, *7*, 394.
(69) Hradetzky, D.; Mueller, C.; Reinecke, H. *J. Opt. A: Pure Appl. Opt*. **2006**, *8*, S360.
(70) Hoffmann, C.; Schmitt, K.; Brandenburg, A.; Hartmann, S. *Anal. Bioanal. Chem.* **2007**, *387*, 1921.
(71) Yuan, W.; Ho, H. P.; Wong, C. L.; Kong, S. K.; Lin, C. L. *IEEE Sens. J.* **2007**, *7*, 70.
(72) Koster, T.; Lambeck, P. *Sens. Actuators, B: Chem.* **2002**, *82*, 213.
(73) Gut, K. *J. Phys. IV* **2005**, *129*, 109.
(74) Stamm, C.; Dangel, R.; Lukosz, W. *Opt. Commun.* **1998**, *153*, 347.
(75) Ayras, P.; Honkanen, S.; Grace, K. M.; Shrouf, K.; Katila, P.; Leppihalme, M.; Tervonen, A.; Yang, X.; Swanson, B.; Peyghambarian, N. *J. Opt. A: Pure Appl. Opt*. **1998**, *7*, 1261.
(76) Kribich, K. R.; Copperwhite, R.; Barry, H.; Kolodziejczyk, B.; Sabattié, J.-M.; O'Dwyer, K.; MacCraith, B. D. *Sens. Actuators, B: Chem*. **2005**, *107*, 188.
(77) Goddard, N. J.; Singh, K.; Hulme, J. P.; Malins, C.; Holmes, R. J. *Sens. Actuators, A: Phys.* **2002**, *100*, 1.
(78) Malins, C.; Fielden, P. R.; Goddard, N. J. *Meas. Sci. Technol.* **2004**, *15*, 948.
(79) Cunningham, B.; Li, P.; Lin, B.; Pepper, J. *Sens. Actuators, B: Chem.* **2002**, *81*, 316.
(80) Challener, W. A.; Edwards, J. D.; McGowan, R. W.; Skorjanec, J.; Yang, Z. *Sens. Actuators, B: Chem.* **2000**, *71*, 42.
(81) Yuen, P. K.; Fontaine, N. H.; Quesada, M. A.; Mazumder, P.; Bergman, R.; Mozdy, E. J. *Lab Chip* **2005**, *5*, 959.
(82) Schueller, O. J. A.; Duffy, D. C.; Rogers, J. A.; Brittain, S. T.; Whitesides, G. M. *Sens. Actuators, A: Phys.* **1999**, *78*, 149.
(83) Morhard, F.; Pipper, J.; Dahint, R.; Grunze, M. *Sens. Actuators, B: Chem.* **2000**, *70*, 232.
(84) St. John, P. M.; Davis, R.; Cady, N.; Czajka, J.; Batt, C. A.; Craighead, H. G. *Anal. Chem.* **1998**, *70*, 1108.
(85) Dubendorfer, J.; Kunz, R. E.; Jobst, G.; Moser, I.; Urban, G. *Sens. Actuators, B: Chem.* **1998**, *50*, 210.
(86) Wiki, M.; Gao, H.; Juvet, M.; Kunz, R. E. *Biosens. Bioelectron.* **2001**, *16*, 37.
(87) Hanel, C.; Gauglitz, G. *Anal. Bioanal. Chem.* **2002**, *372*, 91.
(88) Nikitin, P. I.; Gorshkov, B. G.; Nikitin, E. P.; Ksenevich, T. I. *Sens. Actuators, B: Chem.* **2005**, *111*, 500.
(89) Lambeck, P. V.; van Lith, J.; Hoekstra, H. J. W. M. *Sens. Actuators, B: Chem.* **2006**, *113*, 718.
(90) O'Sullivan, D. W.; Millero, F. J. *Mar. Chem.* **1998**, *60*, 75.
(91) Kimoto, H.; Nozaki, K.; Kudo, S.; Kato, K.; Negishi, A.; Kayanne, H. *Anal. Sci.* **2002**, *18*, 247.
(92) Kaltin, S.; Haraldsson, C.; Anderson, L. G. *Mar. Chem.* **2005**, *96*, 53.
(93) Bandstra, L.; Hales, B.; Takahashi, T. *Mar. Chem.* **2006**, *100*, 24.
(94) De Castro, A. J.; Lerma, A. M.; Lopez, F.; M. Guijarro, M.; Diez, C.; Harnando, C.; Madrigal, J. *Infrared Phys. Technol.* **2007**, *51* (1), 21.
(95) Reyes, F.; Grutter, M.; Jazcilevich, A.; Gonzalez-Oropeza, R. *Atmos. Chem. Phys.* **2006**, *6*, 5339.
(96) Eidelman, N.; Raghavan, D.; Forster, A. M.; Amis, E. J.; Karim, A. *Macromol. Rapid Commun.* **2004**, *285*, 259.
(97) Snively, C. M.; Oskarsdottir, G.; Lauterback, J. *Catal. Today* **2001**, *67*, 357.
(98) Chan, K. L. A.; Kazarian, S. G. *J. Comb. Chem.* **2005**, *7*, 185.
(99) Dessipri, E.; Minopoulou, E.; Chryssikos, G. D.; Gionis, V.; Paipetis, A.; Panayiotou, C. *Eur. Polym. J.* **2003**, *39*, 1533.
(100) Werle, P. *Spectrosc. Acta, Pt. A: Mol. Biomol. Spectrosc.* **1998**, *54*, 197.
(101) Allen, M. G. *Meas. Sci. Technol.* **1998**, *9*, 545.
(102) Linnerud, L.; Kaspersen, P.; Jaeger, T. *Appl. Phys. B* **1998**, *57*, 297.
(103) Werle, P.; Popov, A. *Appl. Opt.* **1999**, *38*, 1494.
(104) Werle, P.; Slemr, F.; Maurer, K.; Kormann, R.; Mucke, R.; Janker, B. *Opt. Lasers Eng.* **2002**, *37*, 101.
(105) Kosterev, A. A.; Tittel, F. K. *IEEE J. Quantum Electron.* **2002**, *38*, 582.
(106) Hvozdara, L.; Pennington, N.; Kraft, M.; Karlowatz, M.; Miziakoff, B. *Vib. Spectrosc.* **2002**, *30*, 53.
(107) Capasso, F.; Gmachl, C.; Paiella, R.; Tredicucci, A.; Hutchinson, A. L.; Sivco, D.; Baillargeon, J. N.; Cho, A. Y. *IEEE J. Sel. Top. Quantum Electron.* **2000**, *6*, 931.
(108) Hvozdara, L.; Gianordoli, S.; Strasser, G.; Schrenk, W.; Unterrainer, K.; Gornik, E.; Murthy, C. S.; Kraft, M.; Pustogow, V.; Mizaikoff, B.; Inberg, A.; Croitoru, N. *Appl. Opt.* **2000**, *39*, 6926.
(109) Sharpe, S. W.; Kelly, J. F.; Hartman, J. S.; Gmachl, C.; Capasso, F.; Sivco, D. L.; Baillargeon, J. N.; Cho, A. Y. *Opt. Lett.* **1998**, *23*, 1396.
(110) Schaden, S.; Haberdorn, M.; Frank, J.; Baena, J. R.; Lendl, B. *Appl. Spectrosc.* **2004**, *58* (6), 667.
(111) Kosterev, A. A.; Curl, R. F.; Tittel, F. K.; Gmachl, C.; Capasso, F.; Sivco, D. L.; Baillargeon, J. N.; Hutchinson, A. L.; Cho, A. Y. *Appl. Opt.* **2000**, *39*, 4425.
(112) Weber, W. H.; Remillard, J. T.; Chase, R. E.; Richert, J. F.; Capasso, R.; Gmachl, C.; Hutchinson, A. L.; Sivco, D. L.; Baillargeon, J. N.; Cho, A. Y. *Appl. Spectrosc.* **2002**, *56*, 706.
(113) Nelson, D. D.; McManus, B.; Urbanski, S.; Herndon, S.; Zahniser, M. S. *Spectrosc. Acta, Pt. A: Mol. Biomol. Spectrosc.* **2004**, *60*, 3325.
(114) Kolhed, M.; Haberkorn, M.; Pustogov, V.; Mizaikoff, B.; Frank J.; Karlberg, B. Lendl, B. *Vib. Spectrosc.* **2002**, *29*, 282.
(115) Tau, S.; Sarma, T. V. S. *Opt. Lett.* **2006**, *31* (10), 1423.
(116) Wu, B., Chang, C.; Sree, U.; Chiu, K.; Lo, J. *Anal. Chim. Acta* **2006**, *576*, 91.
(117) Lin, T.; Sree, R.; Tseng, S.; Chiu, K.; Wu, C.; Lo, J. *Atmos. Environ.* **2004**, *38*, 4111.
(118) Velasco, E.; Lamb, B.; Westberg, H.; Allwine, E.; Sosa, G.; Arriaga-Colina, J. L; Jobson, B. T.; Alexander, M. L.; Prazeller, P.; Knighton, W. B.; Rogers, T. M.; Grutter, M.; Herndon, S. C.; Kolb, C. E.; Zavala, M.; de Foy, B.; Volkamer, R.; Molina, L. T.; Molina, M. J. *Atmos. Chem. Phys.* **2007**, *7*, 329.
(119) Wu, Y.; Zheng, W.; Qu, J. Y. *Opt. Lett.* **2006**, *31* (21), 3122.
(120) Wu, Y.; Qu, J. Y. *J. Biomed. Opt.* **2006**, *11* (5), 054023 1.
(121) Drezek, R.; Brookner, C.; Pavlova, I.; Boiko, I.; Malpica, A.; Lotan, R.; Follen, M.; Richards-Kortum, R. *Photochem. Photobiol.* **2001**, *73*, 636.
(122) Brookner, C. K.; Follen, M. Boiko, I.; Galvan, J.; Thomsen, S.; Malpica, A.; Suzuki, S.; Lotan, R.; Richards-Kortum, R. *Photochem. Photobiol.* **2000**, *71* (6), 730.
(123) Onizawa, K.; Okamura, N.; Saginoya, H.; Yoshida, H. *Oral Oncol.* **2003**, *39*, 150.
(124) Vivian, J. T.; Callis, P. R. *Biophys. J.* **2001**, *80*, 2093.
(125) Monsellier, E.; Bedouelle, H. *Protein Eng. Des. Sel.* **2005**, *18*, 445.
(126) Duy, C.; Fitter, J. *Biophys. J.* **2006**, *90*, 3704.
(127) Patra, D.; Mishra, A. K. *Anal. Bioanal. Chem.* **2002**, *373*, 304.

(128) Ryder, A. G. *J. Fluoresc*. **2004**, *14*, 99.
(129) Sarma, A. K.; Ryder, A. G. *Energy Fuels* **2006**, *20*, 783.
(130) Pouilli, K. I.; Mousdis, G. A.; Georgiou, C. A. *Anal. Bioanal. Chem.* **2006**, *386*, 1571.
(131) Scott, S. M.; James, D.; Ali, Z.; O'Hare, W. T.; Rowell, F. J. *Analyst* **2003**, *128*, 966.
(132) Laserna, J. *An Introduction to Raman Spectroscopy: Introduction and Basic Principles*; Wiley: New York, 2001.
(133) Owen, C. A.; Notingher, I.; Hill, R. *J. Mater. Sci.: Mater. Med.* **2006**, *17*, 1019.
(134) Uzunbajakava, N.; Lenferink, A.; Kraan, Y.; Volokhina, E.; Vrensen, G. Greve, J.; Otto, C. *Biophys. J.* **2003**, *6*, 3698.
(135) Shafer-Peltier, K. E.; Haka, A. S.; Motz, J. T.; Fitzmaurice, M.; Dasari, R. R.; Field, S. *J. Cell Biochem.* **2002**, *39*, 125.
(136) Puppels, G. J. *J. Raman Spectrosc.* **2002**, *7*, 496.
(137) Kneipp, J.; Schut, T. B.; Kliffen, M.; Menke-Pluijmers, M.; Puppels, G. *Vib. Spectrosc*. **2002**, *1*, 67.
(138) Notingher, I.; Green, C.; Dyer, C.; Perkins, E.; Hopkins, N.; Lindsay, C.; Hench, L. L. *J. R. Soc. Interface* **2004**, *1*, 79.
(139) Stuart, D. A.; Biggs, K. B.; Van Duyne, R. P. *Analyst* **2006**, *131*, 568.
(140) Vo-Dinh, T.; Yan, F.; Wabuyele, M. B. Surface-enhanced Raman Scattering: Physics and Application. *Top Appl. Phys.* **2006**, *103*, 409.
(141) Zhang, X.; Shah, N.; Van Duyne, R. P. *Vib. Spectrosc*. **2006**, *42*, 2.
(142) Yonzon, C. R.; Stuart, D. A.; Zhang, X.; McFarland, A. D.; Haynes, C. L.; Van Duyne, R. P. *Talanta* **2005**, *67*, 438.
(143) Stuart, D. A.; Yuen, J. M.; Shah, N.; Lyandres, O.; Yonzon, C.; Glucksberg, M. R.; Walsh, J. T.; Van Duyne, R. P. *Anal. Chem*. **2006**, *78*, 7211.
(144) Deckert, V.; Zeisel, D.; Zenobi, R.; Vo-Dinh, T. *Anal. Chem*. **1998**, *70* (13), 2646.
(145) Chen, K.; Leona, M.; Vo-Dinh, K.; Yan, F.; Wabuyele, M. B.; Vo-Dinh, T. *J. Raman Spectrosc.* **2006**, *37*, 520.
(146) Chen, K.; Vo-Dinh, K.; Yan, F.; Wabuyele, M. B.; Vo-Dinh, T. *Anal. Chim. Acta* **2006**, *569*, 234.
(147) Schmidt, H.; Nguyen, B. H.; Pfannkuche, F.; Amann, H.; Kronfeldt, H. D.; Kowalewska, G. *Mar. Pollut. Bull*. **2004**, *49*, 229.
(148) Lobnik, A. In *Optical Chemical Sensors*; Baldini, F., Chester, A. N., Homola, J., Martellucci, S., Eds.; NATO Science Series 224; Springer: New York, 2006.
(149) Lin, J.; Liu, D. *Anal. Chim. Acta* **2000**, *408*, 49.
(150) Makedonski, P.; Brandes, M.; Grahn, W.; Kowalsky, W.; Wichern, J.; Weise, S.; Johannes, H. *Dyes Pigm.* **2004**, *61*, 109.
(151) Gotou, T.; Noda, M.; Tomiyama, T.; Sembokuya, H.; Kubouchi, M.; Tsuda, K. *Sens. Actuators, B: Chem*. **2006**, *119*, 27.
(152) Segawa, H.; Ohnishi, E.; Arai, Y.; Yoshida, K. *Sens. Actuators, B: Chem*. **2003**, *94*, 276.
(153) Oter, O.; Ertekin, K.; Tapkaya, D.; Alp, S. *Sens. Actuators, B: Chem*. **2006**, *117*, 295.
(154) Baldini, F.; Falai, A.; De Gaudio, A. R.; Landi, D.; Lueger A.; Mencaglia, A.; Scherr, D.; Trettnak, W. *Sens. Actuators, B: Chem*. **2003**, *90*, 132.
(155) Mohr, G. J. *Anal. Bioanal Chem*. **2006**, *386*, 1201.
(156) Mohr, G. *J. Sens. Actuators, B: Chem*. **2005**, *107*. 2.
(157) Wetzl, B. K.; Yarmoluk, S. M.; Craig, D.; Wolfbeis, O. S. *Angew. Chem.* **2004**, *116*, 5515.
(158) Hofelschweiger, B.; Durkop, A.; Wolfbeis, O. S. *Anal. Biochem.* **2005**, *344*, 122.
(159) Suzuki, Y.; Nakano, N.; Suzuki, K. *Environ. Sci. Technol*. **2003**, *37*, 5695.
(160) Kawamura, K.; Kerman, K.; Fujihara, M.; Nagatani, N.; Hashiba, T.; Tamiya, E. *Sens. Actuators, B: Chem*. **2005**, *105*, 495.
(161) Ros-Lis, J.; Martinez-Manez, R.; Rurak, K.; Sancenon, F.; Soto, J.; Spieles, M. *Inorg. Chem*. **2004**, *43*, 5183.
(162) Safavi, A.; Bagheri, M. *Sens. Actuators, B: Chem*. **2004**, 99, 608.
(163) Ros-Lis, J. V.; Martinez-Manez, R.; Soto, J. *Chem. Commun*. **2002**, *19*, 2248.
(164) Badr, I. H. A.; Meyerhoff, M. E. *Anal. Chem*. **2005**, *77*, 6719.
(165) Teshima, N.; Li, J.; Toda, K.; Dasgupta, P. K. *Anal. Chim. Acta* **2005**, *535*, 189.
(166) Carter, J. C.; Alvis, R. M.; Brown, S. B.; Langry, K. C.; Wilson, T. S.; McBride, M. T.; Murick, M. L.; Cox, W. R.; Grove, M. S.; Colston, B. W. *Biosens. Bioelectron*. **2006**, *21*, 1359.
(167) Duong, H. D.; Sohn, O.; Lam, H. T.; Thee, J. I. *Microchem. J.* **2006**, *84*, 50.
(168) Kermis, H. R.; Kostov, Y.; Rao, G. *Analyst* **2003**, *128*, 1181.
(169) Sanchez-Barragan, I.; Costa-Fernandez, J. M.; Sanz-Medel, A.; Valledor, M.; Ferrero, F. J.; Campo, J. C. *Anal. Chim. Acta* **2006**, *562*, 197.
(170) Ando, Y.; Iino, S.; Yamada, K.; Umezawa, K.; Iwasawa, N.; Citterio, D.; Suzuki, K. *Sens. Actuators, B: Chem*. **2007**, *121*, 74.
(171) Le, T. P.; Rogers, J. E.; Kelly, L. A. *J. Phys. Chem A* **2000**, *104*, 6778.
(172) De Silva, A. P.; Rice, T. E. *J. Chem. Soc., Chem. Commun*. **1999**, *2*, *163*.
(173) Li, Z.; Niu, C.; Zeng, G.; Liu, Y.; Gao, P.; Huang, G.; Mao, Y. *Sens. Actuators, B: Chem*. **2006**, *114*, 308.
(174) Higgins, B.; DeGraff, B. A.; Demas, J. N. *Inorg. Chem*. **2005**, *44* (19), 6662.
(175) Chen, X.; Lin, L.; Dai, Y.; Wang, X. *Anal. Chim. Acta* **2004**, *506*, 9.
(176) Mohr, G.; Draxler, S.; Trznadel, K.; Lehmann, F.; Lippitsch, M. E. *Anal. Chim. Acta* **1998**, *360*, 119.
(177) Nivens, D. A.; Schiza, M. V.; Angel, S. M. *Talanta* **2002**, *58*, 543.
(178) Mills, A.; Eaton, K. *Quim Anal.* **2000**, *19*, 75.
(179) Wolfbeis, O. S.; Klimant, I.; Werner, T.; Huber, C.; Kosch, U.; Krause, C.; Neurauter, G.; Durkop, A. *Sens. Actuators, B: Chem*. **1998**, 51, 17.
(180) Cajlakovic, M.; Bizzarri, A.; Ribitsch, V. *Anal. Chim. Acta* **2006**, *573*−*574*, 57.
(181) Zhu, Q.; Aller, R. C.; Fan, Y. *Mar. Chem*. **2006**, *101*, 40.
(182) Amao, Y. *Microchim. Acta* **2003**, *143*, 1.
(183) Amao, Y.; Okura, I.; Miyashita, T. *Bull. Chem. Soc. Jpn*. **2001**, *74*, 1156.
(184) Fujiwara, Y.; Okura, I.; Miyashita, T.; Amao, Y. *Anal. Chim. Acta* **2002**, *471*, 25.
(185) Choi, S. J.; Choi, B. G.; Park, S. M. *Anal. Chem*. **2002**, *74* (9), 1998.
(186) Fuller, Z. J.; Bare, W. D.; Kneas, K. A.; Xu, W. Y.; Demas, J. N.; DeGraaf, B. A. *Anal. Chem*. **2003**, *75* (11), 2670.
(187) McDonagh, C.; Bowe, P.; Mongey, K.; MacCraith, B. D. *J. Non-Cryst. Solids* **2002**, *306*, 138.
(188) Lee, S. K.; Okura, I. *Anal. Commun*. **1997**, *34*, 185.
(189) Kerry, J. P.; Papkovsky, D. P. *Research Advances in Food Science*; Global Research Network: Kerala, India, 2002; Vol. 3, p 121.
(190) O'Mahony, F. C.; O'Riordan, T. C.; Papkovskaia, N.; Kerry, J. P.; Papkovsky, D. B. *Food Control* **2006**, *17*, 286.
(191) O'Riordan, T. C.; Voraberger, H.; Kerry, J. P.; Papkovsky, D. B. *Anal. Chim. Acta* **2005**, *530*, 135.
(192) Glenn, S. J.; Cullum, B. M.; Nair, R. B.; Nivens, D. A.; Murphy, C. J.; Angel, S. M. *Anal. Chim. Acta* **2001**, *448*, 1.
(193) Bedoya, M.; Diez, M. T.; Moreno-Bondi, M. C.; Orellana, G. *Sens. Actuators, B: Chem*. **2006**, *113*, 573.
(194) McGaughey, O.; Ros-Lis, J. V.; Guckian, A.; McEvoy, A. K.; McDonagh, C.; MacCraith, B. D. *Anal. Chim. Acta* **2006**, *570*, 15.
(195) Xu, C.; Qin, Y.; Bakker, E. *Talanta* **2004**, *63*, 180.
(196) Quinti, L.; Allen, N. S.; Edge, M.; Murphy, B. P.; Perotti, A. *J. Photochem. Photobiol. A: Chem*. **2003**, *155*, 79.
(197) Ng, S. M.; Narayanaswamy, R. *Anal. Bioanal. Chem.* **2006**, *386*, 1235.
(198) Baduaga, R.; Lakowicz, J. R.; Geddes, C. D. *Anal. Chim. Acta* **2004**, *522*, 9.
(199) Huber, C.; Klimant, I.; Krause, C.; Werner, T.; Wolfbeis, O. S. *Anal. Chim. Acta* **2001**, *449*, 81.
(200) Wright, J. D.; Sommerdijk, N. A. *Sol-gel Materials: Chemistry and Application*; CRC Press: Boca Raton, 2000.
(201) MacCraith, B. D.; McDonagh, C. *J. Fluoresc*. **2002**, *12* (3,4), 333.
(202) Tao, Z.; Tehan, E. G.; Tang, Y.; Bright, F. V. *Anal. Chem*. **2006**, *78*, 1939.
(203) Bukowski, R. M.; Ciriminna, R.; Pagliaro, M.; Bright, F. V. *Anal. Chem*. **2005**, *77*, 2670.
(204) Bukowski, R. M.; Davenport, M. D.; Titus, A. H.; Bright, R.V. *Appl. Spectrosc.* **2006**, *60* (9), 951.
(205) Klimant, I.; Ruckruh, F.; Liebsch, G.; Stangelmayer, A.; Wolfbeis, O. S. *Mikrochim. Acta* **1999**, *131*, 35.
(206) Holder, E.; Oelkrug, D.; Egelhaaf, H.; Mayer, H. A.; Lindner, E. *J. Fluoresc*. **2002**, *12* (3,4), 383.
(207) Zhang, H.; Li, B.; Lei, B.; Li, W.; Lu, S. *Sens. Actuators, B: Chem*. **2007**, *12* (1), 208.
(208) Von Bultzingslowen, C.; McEvoy, A.; McDonagh, C.; MacCraith, B. D. *Anal. Chim. Acta* **2003**, *480*, 275.
(209) Von Bultzingslowen, C.; McEvoy, A.; McDonagh, C. M.; MacCraith, B. D.; Klimant, I.; Krause, C.; Wolfbeis, O. S. *Analyst* **2002**, *127*, 1478.
(210) Grosso, D.; Cagnol, F.; Soler-Illia, G. J.; Crepaldi, E. L.; Amenitsch, H.; Brunet-Bruneau, A.; Bourgeois, A.; Sanchez, C. *Adv. Funct. Mater*. **2004**, *14*, 309.
(211) Nicole, L.; Boissiere, C.; Grosso, D.; Hesemann, P.; Moreau, J.; Sanchez, C. *Chem. Commun.* **2004**, *20*, 2312.
(212) Lei, B.; Li, B.; Zhang, H.; Lu, S.; Zheng, Z.; Li, W.; Wang, Y. *Adv. Funct. Mater*. **2006**, *16*, 1883.
(213) Tao, S.; Winstead, C. B.; Jindal, R.; Singh, J. P. *IEEE Sens. J*. **2004**, *4* (3), 322.
(214) Zhang, P.; Guo, J.; Wang, Y.; Pang, W. *Mater. Lett*. **2002**, *53*, 400.
(215) Mills, A. *Sens. Actuators, B: Chem*. **1998**, *51*, 60.
(216) Reiss, J. G.; Krafft, M. P. *Biomaterials* **1998**, *19*, 1529.
(217) Voraberger, H. S.; Kreimaier, H.; Biebernik, K.; Kern, W. *Sens. Actuators, B: Chem*. **2001**, *74*, 179.

(218) Florescu, M.; Katerkamp, A. *Sens. Actuators, B: Chem.* **2004**, *97*, 39.
(219) Holmes-Smith, A. S.; Zheng, X.; Uttamial, M. *Meas. Sci. Technol.* **2006**, *17*, 3328.
(220) Neurauter, G.; Klimant, I.; Wolfbeis, O. S. *Fresnius J. Anal. Chem.* **2000**, *366*, 481.
(221) Ge, X.; Kostov, Y.; Rao, G. *Biosens. Bioelectron.* **2003**, *18*, 857.
(222) Waldner, A.; Barnard, S. M. U.S. Patent 6,338,822, 2002.
(223) Schroder, C. R.; Klimant, I. *Sens. Actuators, B: Chem.* **2005**, *107*, 572.
(224) Haupt, K.; Mosback, K. *Chem. Rev.* **2000**, *100*, 2495.
(225) Chen, Y.; Brazier, J. J.; Yan, M.; Bargo, P. R.; Prahl, S. A. *Sens. Actuators, B: Chem.* **2004**, *102*, 107.
(226) Lieberzeit, P. A.; Gazda-Miarecka, S.; Halikias, K.; Schirk, C.; Kauling, J.; Dickert, F. L. *Sens. Actuators, B: Chem.* **2005**, *1112*, 259.
(227) Al-Kindy, S.; Badia, R.; Suarez-Rodriguez, J. L.; Diaz-Garcia, M. E. *Crit. Rev. Anal. Chem.* **2000**, *30* (4), 291.
(228) Kindschy, L. M.; Alocilya, E. C. *Trans. ASAE* **2004**, *47* (4), 1375.
(229) Orellana, G.; Garcia-Fresnadillo, D. In *Optical sensors: industrial, environmental, and diagnostic applications*; Narayanaswamy, R., Wolfbeis, O. S., Eds.; Springer: New York, 2004; p 338.
(230) Mongey, K. F.; Vos, J. G.; MacCraith, B. D.; McDonagh, C.; Coates, C.; McGarvey, J. J. *J. Mater. Chem.* **1997**, *7*, 1473.
(231) Steinberg, I. M.; Lobnik, A.; Wolfbeis, O. S. *Sens. Actuators, B: Chem.* **2003**, *90*, 230.
(232) Orellana, G.; Moreno-Bondi, M. C.; Garcia-Fresnadillo, D.; Marazuela, M. D. In *Frontiers in Chemical Sensors: Novel Principles and Techniques*; Orellano, G., Wolfbeis, O.O., Eds.; Springer: New York, 2005; p 189.
(233) Roth, T. P. Ph.D. Thesis, Swiss Federal Institute of Technology, 2001.
(234) Tao, S.; Gong, S.; Fanguy, J. C.; Hu, X. *Sens. Actuators, B: Chem.* **2007**, *120*, 724.
(235) Safafi, A.; Banazadeh, A. R. *Anal. Chim. Acta* **2007**, *583*, 326.
(236) Amao, Y.; Komori, T. *Talanta* **2005**, *66*, 976.
(237) Nakamura, N.; Amao, U. *Sens. Actuators, B: Chem.* **2003**, *92*, 98.
(238) Miled, O. B.; Grosso, D.; Sanchez, C.; Livage, J. *J. Phys. Chem. Solids* **2004**, *65*, 1751.
(239) Oter, O.; Ertekin, K.; Topkaya, D.; Alp, S. *Sens. Actuators, B: Chem.* **2006**, *117*, 295.
(240) Oter, O.; Ertekin, K.; Topkaya, D.; Alp, S. *Anal. BioAnal. Chem.* **2006**, *386*, 1225.
(241) Chu, C.; Lo, Y. *Sens. Actuators, B: Chem.* **2007**, *124* (2), 376.
(242) Tang, Y.; Tao, Z.; Bukowski, R. M.; Tehan, E. C.; Karri, S.; Titus, A. H.; Bright, F. V. *Analyst* **2006**, *131*, 1129.
(243) Fernandez-Sanchez, J. F.; Cannas, R.; Spichiger, S.; Steiger, R.; Spicher-Keller, U. E. *Anal. Chim. Acta* **2006**, *566*, 271.
(244) Derinkuyu, A.; Ertekin, K.; Oter, O.; Denizalti, S.; Cetinkaya, E. *Anal. Chim. Acta* **2007**, *588*, 42.
(245) Citterio, D.; Takeda, J.; Kosugi, M.; Hisamoto, H.; Sasaki, S.; Komatsu, H.; Suzuki, K. *Anal. Chem.* **2007**, *79*, 1237.
(246) Barauh, M.; Qin, W.; Vallee, R. A. L.; Beljonne, D.; Rohand, R.; Dehaen, W.; Boens, N. *Org. Lett.* **2005**, *7* (20), 4377.
(247) Ligler, F. S.; Sapsford, K. W.; Golden, J. P.; Shriver-Lake, L. C.; Taitt, C. R.; Dyer, M. A.; Baraone, S.; Myatt, C. J. *Anal. Sci.* **2007**, *23*, 5.
(248) Taitt, C. R.; Anderson, G. P.; Lingerfelt, B. M.; Feldstein, M. J.; Ligler, F.S. *Anal. Chem.* **2002**, *74*, 6114.
(249) Sapsford, K. E.; Taitt, C. R.; Loo, N.; Ligler, F. S. *Appl. Environ. Microbiol.* **2005**, *71*, 5590.
(250) Shriver-Lake, L. C.; Ligler, F. S. *IEEE Sens. J.* **2005**, *5* (4), 751.
(251) Qin, W. W.; Baruah, M.; De Borggraeve, W. M.; Boens, N. *J. Photochem. Photobiol. A: Chem.* **2006**, *183*, 190.
(252) Kuwana, E.; Liang, F.; Sevick-Muraca, E. M. *Biotechnol. Prog.* **2004**, *20*, 1561.
(253) Ryder, A. G.; Power, S.; Glynn, T. J. *Appl. Spectrosc.* **2003**, *57*, 73.
(254) Hradil, J.; Davis, C.; Mongey, K.; McDonagh, C.; MacCraith, B. D. *Meas. Sci. Technol.* **2002**, *13*, 1552.
(255) Kostov, Y.; Rao, G. *Rev. Sci. Instrum.* **2003**, *74*, 4129.
(256) Chodavarapu, V. P.; Shubin, D. O.; Bukowski, R. M.; Titus, A. H.; Cartwright, A. N.; Bright, F. V. *IEEE Trans. Circuits Syst. I: Regul. Pap.* **2007**, *54*, 111.
(257) Kostov, Y.; Rao, G. *Sens. Actuators, B: Chem.* **2003**, *90*, 139.
(258) Ogurtsov, V. I.; Papkovsky, D. B. *Sens. Actuators, B: Chem.* **2006**, *113*, 917.
(259) O'Mahony, F. C.; O'Riordan, T. C.; Papkovskaia, N.; Ogurtsov, V. I.; Kerry, J. P.; Papkovsky, D. B. *Packag. Technol. Sci.* **2004**, *17*, 225.
(260) Shinar, R.; Zhou, Z. Q.; Choudhury, B.; Shinar, J. *Anal. Chim. Acta* **2006**, *568*, 190.
(261) Neurauter, G.; Klimant, I.; Wolfbeis, O. S. *Anal. Chim. Acta* **1999**, *382*, 67.
(262) Huber, C.; Klimant, I.; Krause, C.; Werner, T.; Mayr, T.; Wolfbeis, O. S. *Fresenius J. Anal. Chem.* **2000**, *368*, 196.
(263) Borisov, S. M.; Krause, C.; Arain, S.; Wolfbeis, O. S. *Adv. Mater.* **2006**, *18*, 1511.
(264) Stahl, H.; Glud, A.; Schroder, C. R.; Klimant, I.; Tengberg, A.; Glud, R. N. *Limnol. Oceanogr. Meth.* **2006**, *4*, 336.
(265) Liebsch, G.; Klimant, I.; Krause, C.; Wolfbeis, O. S. *Anal. Chem.* **2001**, *73*, 4354.
(266) Huber, C.; Klimant, I.; Krause, C.; Werner, T.; Wolfbeis, O. S. *Anal. Chim. Acta* **2001**, *449*, 81.
(267) Mayr, T.; Klimant, I.; Wolfbeis, O. S.; Werner, T. *Anal. Chim. Acta* **2002**, *462*, 1.
(268) Borisov, S. M.; Neurauter, G.; Schroeder, C.; Klimant, I.; Wolfbeis, O. S. *Appl. Spectrosc.* **2006**, *60*, 1167.
(269) Rowe, H. M.; Chan, S. P.; Demas, J. N.; DeGraff, B. A. *Appl. Spectrosc.* **2003**, *57*, 532.
(270) Aslan, K.; Gryczynski, I.; Malicka, J.; Matveeva, E.; Lakowicz, J. R.; Geddes, C. D. *Curr. Opin. Biotechnol.* **2005**, *16*, 55.
(271) Lakowicz, J. R. *Anal. Biochem.* **2005**, *337*, 171.
(272) Stranik, O.; McEvoy, H. M.; McDonagh, C.; MacCraith, B. D. *Sens. Actuators, B: Chem.* **2005**, *107*, 148.
(273) Zhang, J.; Lakowicz, J. R. *Opt. Express* **2007**, *15*, 2598.
(274) Sirbuly, D. J.; Tao, A.; Law, M.; Fan, R.; Yang, P. D. *Adv. Mater.* **2007**, *19*, 61.
(275) Arnold, S.; Khoshsima, M.; Teraoka, I.; Holler, S.; Vollmer, F. *Opt. Lett.* **2003**, *28*, 272.
(276) Hanumegowda, N. M.; White, I. M.; Oveys, H.; Fan, X. D. *Sens. Lett.* **2005**, *3*, 315.
(277) White, I. M.; Zhu, H. Y.; Suter, J. D.; Hanumegowda, N. M.; Oveys, H.; Zourob, M.; Fan, X. D. *IEEE Sens. J.* **2007**, *7*, 28.
(278) Camargo, E. A.; Chong, H. M. H.; De La Rue, R. M. *Appl. Opt.* **2006**, *45*, 6507.
(279) Thrush, E.; Levi, O.; Cook, L. J.; Deich, J.; Kurtz, A.; Smith, S. J.; Moerner, W. E.; Harris, J. S. *Sens. Actuators, B: Chem.* **2005**, *105*, 393.
(280) Cristea, D.; Craciunoiu, F.; Modreanu, M.; Caldararu, M.; Cernica, I. *Opt. Mater.* **2001**, *17*, 201.
(281) Adams, M. L.; Enzelberger, M.; Quake, S.; Scherer, A. *Sens. Actuators, A: Phys.* **2003**, *104*, 25.
(282) Medintz, I. L.; Clapp, A. R.; Mattoussi, H.; Goldman, E. R.; Fisher, B.; Mauro, J. M. *Nat. Mater.* **2003**, *2*, 630.
(283) Wang, X. J.; Ruedas-Rama, M. J.; Hall, E. A. H. *Anal. Lett.* **2007**, *40*, 1497.
(284) Costa-Fernandez, J. M.; Pereiro, R.; Sanz-Medel, A. *Trac-Trends Anal. Chem.* **2006**, *25*, 207.
(285) Blue, R.; Kent, N.; Polerecky, L.; McEvoy, H.; Gray, D.; MacCraith, B. D. *Electron. Lett.* **2005**, *41*, 682.
(286) Holthoff, W. G.; Tehan, E. C.; Bukowski, R. M.; Kent, N.; MacCraith, B. D.; Bright, F. V. *Anal. Chem.* **2005**, *77*, 718.
(287) Ruckstuhl, T.; Seeger, S. *Appl. Opt.* **2003**, *42*, 3277.
(288) Sauer, U.; Preininger, C.; Krumpel, G.; Stelzer, N.; Kern, W. *Sens. Actuators, B: Chem.* **2005**, *107*, 178.

CR068102G